Accepted Article

Diadenosine tetraphosphate (Ap4A) – an *E. coli* alarmone or a damage metabolite?

Dragana Despotović[1], Alexander Brandis[2], Alon Savidor[3], Yishai Levin[3], Laura Fumagalli[4] and Dan S. Tawfik[1*]

Running title: Ap4A – an *E. coli* alarmone or damage metabolite?

[1]Department of Biomolecular Sciences, Weizmann Institute of Science, Rehovot 76100, Israel.

[2]Life Sciences Core Facilities, Weizmann Institute of Science, Rehovot 76100, Israel.

[3]Nancy and Stephen Grand Israel National Center for Personalized Medicine, Weizmann Institute of Science, Rehovot 76100, Israel.

[4]Dipartimento di Scienze Farmaceutiche, Università degli Studi di Milano, via Mangiagalli 25, I-20133, Milano, Italy.

[*]Corresponding author: Dan S. Tawfik

E-mail: dan.tawfik@weizmann.ac.il (D.S.T.)

Phone: +972 8 934-3637

This article has been accepted for publication and undergone full peer review but has not been through the copyediting, typesetting, pagination and proofreading process, which may lead to differences between this version and the Version of Record. Please cite this article as doi: 10.1111/febs.14113
This article is protected by copyright. All rights reserved.

Article type : Original Article

Abbreviations: AARS – aminoacyl-tRNA synthetase; Ap4A – diadenosine tetraphosphate; CAP – chloramphenicol, CBS - cysthathionine β-synthase domain; IMP – inosine monophosphate; IMPDH – inosine monophosphate dehydrogenase; M9-Glc – M9 minimal medium with 0.4 % of glucose; (p)ppGpp – guanosine pentaphosphate/tetraphosphate; XMP - xanthosine monophosphate

Abstract

Under stress, metabolism is changing: specific up- or down-regulation of proteins and metabolites occurs as well as side-effects. Distinguishing specific stress-signaling metabolites (alarmones) from side-products (damage metabolites) is not trivial. One example is diadenosine tetraphosphate, Ap4A – a side-product of aminoacyl-tRNA synthetases found in all domains of life. The earliest observations suggested that Ap4A serves as an alarmone for heat stress in *E. coli*. However, despite 50 years of research, the signaling mechanisms associated with Ap4A remain unknown. We defined a set of criteria for distinguishing alarmones from damage metabolites to systematically classify Ap4A. In a nutshell, no indications for a signaling cascade that is triggered by Ap4A were found; rather, we found that Ap4A is efficiently removed in a constitutive, non-regulated manner. Several-fold perturbations in Ap4A concentrations have no effect, yet accumulation at very high levels is toxic due to disturbance of zinc homeostasis, and also because Ap4A's structural overlap with ATP can result in spurious binding and inactivation of ATP binding proteins. Overall, Ap4A met all criteria for a damage metabolite. While we do not exclude any role in signaling, our results indicate that the damage metabolite option should be considered as the null hypothesis when examining Ap4A and other metabolites whose levels change upon stress.

This article is protected by copyright. All rights reserved.

Accepted Article

Keywords: diadenosine tetraphosphate, damage metabolite, alarmone, *E. coli*

Accepted Article

Introduction

Metabolites are small, natural organic molecules. The vast majority of metabolites take part in catabolic and anabolic reactions, while others serve to initiate signaling cascades, as secondary messengers, including alarmones. In bacteria, alarmone production is induced during stress (*e.g.*, starvation, heat, oxidative stress) and their presence activates adequate cellular responses [1,2]. In most cases, secondary messengers comprise specific metabolites with no additional roles. However, metabolites with dual roles are also known, including NAD – an essential enzymatic cofactor that also acts as a signaling molecule in regulating transcription, apoptosis and DNA repair [3]. In recent years, another class of metabolites, damage metabolites, has attracted considerable attention [4,5]. Damage metabolites are side-products of enzymatic reactions, or products of non-enzymatic breakdown of other metabolites. Their accumulation can be deleterious, and thus, enzymatic pathways that convert them into harmless products have evolved. Under stress, damage metabolites may accumulate more rapidly, and their effects on cell growth and viability may become pronounced [6]. However, not every side-product is a damage metabolite, and not every metabolite whose concentration rises under stress is an alarmone. Distinguishing between side-effects and specifically induced effects of stress is not trivial. For example, increased mutation rates under stress have been proposed to be adaptive [7], but high mutation rates can also be a mere side-effect of stress [8].

Diadenosine tetraphosphate (Ap4A) is the example of a metabolite that could belong to either category – damage metabolite, or alarmone. Discovered 50 years ago [9], this molecule remains a mystery. Ap4A is generated as a side-product of aminoacyl-tRNA synthetases

This article is protected by copyright. All rights reserved.

(AARS) [10], by ATP reacting with the amino-acid-AMP intermediate, or directly, via reaction of two ATPs [11]. During normal growth, *in vivo* concentrations of Ap4A seem to vary widely from 0.05-1 µM in mammalian cells [12] to 1-3 µM in bacteria [13]. These relatively low concentrations (< 10^3-fold lower than ATP) are the outcome of Ap4A hydrolases, and/or Ap4A phosphorylases (where phosphate acts as nucleophile instead of water), seen in all kingdoms of life. In *E. coli*, Ap4A concentrations were reported to respond to external stimuli such as heat [14], oxidative stress [15,16], and ethanol [17]. These observations led to the hypothesis that Ap4A functions as an alarmone [15,18]. Throughout the years, Ap4A has been linked to a wide range of key biological functions ranging from heat-stress response in *E. coli* [14] to mammalian tear secretion [19] and is described in > 500 research reports. However, to date, no signaling pathways that are specifically triggered by Ap4A are known, certainly not in bacteria. On the other hand, knockout of Ap4A hydrolase (ApaH) results in high Ap4A levels, increased sensitivity to heat and starvation [20], weakened stress-induced mutagenesis response [21], decreased persister formation [22] and inhibit sporulation [16].

Two hypotheses should be therefore considered: (i) Ap4A is an alarmone with specific signaling and/or regulatory roles in stress, or (ii) Ap4A is a damage metabolite. These hypotheses are not necessarily mutually exclusive – Ap4A may have emerged as damage metabolite, and mechanisms for its removal have consequently evolved, but it may had also been recruited in some organisms for specific signaling. To assign Ap4A, or any metabolite, to one category or another, it is necessary to establish specific criteria.

This article is protected by copyright. All rights reserved.

Accepted Article

Accepted Article

An alarmone and/or a secondary messenger should meet the following criteria:

1. Alarmone levels must be regulated such that basal levels persist during ambient conditions and a transient concentration change is triggered by stress [23].

2. An increase in concentration under stress is not indicative in itself. Rather, alarmone levels are controlled via production and/or degradation, whereby the corresponding enzymes are regulated, transcriptionally and/or at the protein level, in response to specific triggers [24,25].

3. Alarmone production and/or degradation via an artificially regulated enzyme would affect growth, under normal conditions and/or stress [26–28].

4. Transcription factors or allosteric enzymes are found that are selectively modulated by the alarmone. These regulated proteins would be associated with other proteins whose levels change when alarmone levels change (*e.g.* via transcriptional regulation networks) [29].

Not all criteria must be fulfilled. For example, changes in NAD levels are not induced as such, but they are sensed and can initiate a signaling cascade. Thus, while criterion 1 is irrelevant for NAD, criterion 4 has been met [30].

On the other hand, distinct criteria of damage metabolites include:

5. It is a side-product of a metabolic enzyme rather than being produced by a dedicated enzyme that is accordingly regulated [31].

6. Enzyme(s) that degrade damage metabolites exist and degradation is constitutive rather then regulated [32].

This article is protected by copyright. All rights reserved.

7. The damage metabolite can accumulate to some degree with no physiological effects yet become toxic upon exceeding a certain threshold, especially under stress. Accordingly, removal of a damage-metabolite degrading enzyme(s) is deleterious but not lethal [33].

We attempted to systematically examine these criteria, using *E. coli* as a case study. We found that Ap4A is constitutively removed - its degradation is not regulated, neither transcriptionally nor at the enzyme level (criteria 1 and 2 not met). Artificially induced production, or complete degradation of the Ap4A, had no growth effect (criteria 3 not met) and proteins that sense and respond to change in Ap4A cellular level were not identified (criteria 4 not met). On the other hand, Ap4A is a side-product of essential, metabolic enzymes, and its homeostasis is maintained by a constitutively expressed Ap4A hydrolase (criteria 5 and 6 fulfilled). Ap4A becomes toxic but not lethal, only when its concentration rises dramatically, and even then, only under stress conditions (criterion 7 fulfilled). Overall, Ap4A does not fit any of the alarmone criteria, while all damage metabolite criteria are fulfilled. The criteria and tools developed here, foremost, the laboratory sub-functionalization of *E. coli*'s lysyl tRNA-synthetase (LysRS) to generate an Ap4A synthetase - can be applied to decipher the role of Ap4A, and of other stress-related metabolites, in other organisms.

Results

Ap4A hydrolase (ApaH) deficient strains

The only currently available way of perturbing Ap4A levels has been via knockout of *E. coli's* Ap4A hydrolase (ApaH), a symmetrical hydrolase which generates two ADP molecules and belongs to the Nudix superfamily [34,35]. Several phenotypes associated with the *apaH* knockout have been reported, but their mechanistic basis remains unknown.

This article is protected by copyright. All rights reserved.

Accepted Article

Specifically, the *apaH* knockout was reported to have intracellular Ap4A levels that are ~100-fold higher than wild-type and increased sensitivity to stress [20–22].

We constructed a series of *apaH* genetic constructs, aiming to ensure that the observed *ΔapaH* phenotypes are a direct outcome of increased Ap4A concentration and not due to other, unknown secondary functions of ApaH (Table 1). The level of Ap4A in the *ΔapaH* strain, measured by LC-MS, during growth in minimal medium (M9 with 0.4 % glucose; M9-Glc) increased ~350-fold, from 0.2 µM in wild-type to 65 µM in *ΔapaH* (Table 1). In rich media, the *E. coli* K12 *ΔapaH* strain exhibited the same maximal growth rate as the parental, wild-type strain, also upon serial transfer of exponentially growing cultures (Fig 1A and 1B). However, when cells grown in LB medium were transferred to minimal medium, the growth yield was lower in *ΔapaH* (Fig 1C). Accordingly, transfer of *ΔapaH* cells grown to stationary phase in minimal medium to fresh minimal medium led to a longer lag phase (Fig 1D). Additionally, as previously reported, growth in rich medium at 46 °C was almost completely inhibited in *ΔapaH* and cells exhibited an elongated morphology (Fig 1E and 1F). However, cell death was not observed, at least within the first 3 h of incubation at 46 °C (Table 2). As described later, we also compared the proteome of the *apaH* knockout to wild-type, aiming to uncover which proteins are up- or down-regulated at elevated Ap4A levels.

Regulation of ApaH

Following the *apaH* knockout characterization, we replaced the endogenous ApaH with various Ap4A hydrolase variants, chromosomally encoded and expressed under different promoters (Table 1). The *S. cerevisiae* Ap4A phosphorylase, Apa2, was placed under the *apaH* promoter. Apa2 belongs to the HIT (histidine triad) superfamily. It is not a hydrolase, but rather an asymmetrical phosphorylase, generating ATP and ADP from Ap4A and phosphate, and shows no homology in structure, or sequence, to *E. coli*'s ApaH. Both growth

This article is protected by copyright. All rights reserved.

Accepted Article

inhibition at 46 ºC (Fig 2A) and the longer lag time in minimal medium (Fig 2B) of the *apaH* knockout were complemented by *apa2*. Accordingly, the cellular level of Ap4A was restored, to a level that is ≥10-fold lower than wild-type and below the detection limit of our assay (Table 1). Complementation by an enzyme that shares nothing but ApaH's ability to remove Ap4A suggests that the observed *ΔapaH* phenotype relates directly to elevated Ap4A levels, and not any secondary functions of ApaH. Further, if Ap4A has some signaling role in heat-stress and/or starvation, unregulated removal should have an effect. However, regulation (allosteric via a small molecule, or by an *E. coli* protein regulator) is unlikely to be recapitulated by the evolutionarily and biochemically unrelated Apa2.

Furthermore, upon analyzing ApaH, we found that it exhibits low thermostability ($T_M \approx 50$ °C). This low melting point could relate to signaling of higher environmental temperatures. To examine this option, we engineered a thermostable variant of ApaH using computational design [36]. We generated an ApaH variant carrying 29 mutations and exhibiting a T_M of 64 °C, well above the observed heat-stress phenotype at 46 °C (mutations are listed in Material and Methods section). However, genomic complementation of the endogenous ApaH with this variant, ApaH_D7, showed wild-type-like behavior including at 46 °C (Fig 2A and 2B). Thus, as indicated by the Apa2 complementation, ApaH regulation at the enzyme level is unlikely.

We also tested complementation by ApaH mutants with impaired activity to detect the concentration threshold of Ap4A above which phenotypes are observed (Fig 2A and 2B). Active-site mutations may also cause misfolding and loss of protein, as we observed with the ApaH mutants. Thus, we used the stabilized ApaH_D7 variant to introduce two active-site mutations, H120A and H227A. Both of these mutants produced soluble, folded proteins, yet H120A was essentially inactive, while the Ap4A hydrolyzing activity of H227A decreased by 240-fold compared to wild-type ApaH. Complementation with the enzymatically inactive

This article is protected by copyright. All rights reserved.

Accepted Article

ApaH-H120A resulted in a phenotype indistinguishable from the knockout strain, *ΔapaH*. The ApaH-H227A mutant resulted in growth inhibition that is slightly weaker than the *apaH* knockout (Fig 2A and 2B) although its Ap4A level was similar to that of *ΔapaH* (Table 1). Since the cellular Ap4A concentrations were compared on the basis of the culture's optical density and dry cell weight, it may well be that the actual Ap4A levels differ due to different cellular morphology.

Replacement of not only of the hydrolase itself (Apa2 instead of ApaH), but also of its transcriptional regulation, had no effect either. Specifically, we generated constructs expressing Apa2 in the pZA vector – a low copy number plasmid with expression under the anhydrotetracycline (AHT) promoter. This construct was expressed in both the *ΔapaH* and the parental strain, alongside a control construct bearing an inactive Apa2 mutant (Apa2-H161A). Expression of Apa2 or its inactive variant in the parental strain had no effect on growth in LB medium at 46 °C (Fig 3A). The growth rate of the Apa2 complemented *ΔapaH* strain in either LB medium at 46 °C, or in minimal medium at 37 °C, was identical to the parental K12 strain as long as the inducer, AHT, was present, while *ΔapaH* cells expressing the inactive Apa2 mutant behaved as the *ΔapaH* strain (Fig 3B and 3C).

The above results indicated that *E. coli* growth rate is not affected by replacement its endogenous Ap4A hydrolase by another enzyme that removes Ap4A (Apa2). However, small differences cannot be detected by parallel growth and monitoring absorbance. We thus performed a direct growth competition between a K12 strain expressing yeast Apa2 (in addition to the endogenous ApaH) and an identical control strain expressing an inactive Apa2 mutant. Expression of active Apa2 resulted in non-regulated removal of Ap4A, and to levels below detection (in oppose to ~0.2 μM in the parental K12 strain). To quantify the ratio of the competing versus the control cells, the competing strain contained a chloramphenicol resistance marker. The effect of chloramphenicol marker was determined by competing K12

This article is protected by copyright. All rights reserved.

Accepted Article

strains with and without it (both expressing inactive Apa2). The direct competition experiment also indicated no significant growth advantage or disadvantage of Ap4A non-regulated removal neither in LB (Fig 3D) nor in M9-Glc medium (Fig 3E).

Overall, it appears that ApaH's function is not regulated, neither at the enzyme level nor transcriptionally, and certainly not under the conditions tested here; thus, criteria 1 and 2 are not fulfilled. Further, Ap4A levels in the strain expressing yeast Apa2 were significantly reduced – ≤ 0.02 μM, compared to 0.2 μM in the wild-type (Table 1), yet within the perturbation range expected for a signaling molecule. If Ap4A has a signaling role, altered regulation and degradation kinetics should both have some effect (criterion 3 not fulfilled). The above results are, however, entirely consistent with Ap4A being a damage metabolite that is constitutively removed (criterion 6 met). Its accumulation at low levels has no effect, while very high levels (≥ 100-fold compared to wild-type) inhibit growth, but only under challenging conditions and without causing cell death (criterion 7 met).

LysU does not affect the presumed Ap4A-triggered phenotypes

If degradation of Ap4A is not regulated, perhaps synthesis is. Lysyl-tRNA synthetases (LysRS) is considered the main producer of Ap4A in *E. coli*, with two isoforms, LysS and LysU [37]. LysS is constitutively expressed and is likely to be responsible for house-keeping aminoacylation. LysU's expression is thought to be triggered by heat stress, and it has thus been suggested to act primarily as an Ap4A synthetase [38,39]. A *lysU* deletion strain (*ΔlysU*) was reported to grow normally at low temperature (28 °C) but poorly at 44 °C, and this growth defect was ascribed to disruption of Ap4A-mediated heat stress signaling [37]. Further, *E. coli* cells evolved to grow at high temperature exhibited elevated *lysU* levels, and its deletion rendered them thermosensitive [40]. However, a later publication reported that *lysU* deletion has no effect on growth at high temperature [41]. Given these conflicting

This article is protected by copyright. All rights reserved.

Accepted Article

reports, we tested the Δ*lysU* phenotype. In *E. coli* K12, we could not identify any significant growth difference, or any other observable phenotype, upon deletion of *lysU*, including at elevated growth temperatures. Further, the *ΔlysU* and the *ΔlysS* strains showed the very same growth rates at ambient and high temperatures in both rich and minimal media.

Laboratory sub-functionalization of LysRS to generate an Ap4A synthetase

An enzyme whose primary function is Ap4A synthesis is not known, neither in *E. coli* nor in other organisms. However, in nature, secondary, moonlighting functions often evolve to become the primary function of a duplicated, paralogue gene (sub-functionalization) [42]. We engineered a sub-funtionalized LysU variant that produced Ap4A yet had no aminoacylation function.

We established an assay for Ap4A synthetase activity in crude cell lysates based on luminescent detection of ATP generated upon Ap4A hydrolysis. By combining screens of gene libraries and site-directed mutagenesis, we generated a LysU variant capable of executing only Ap4A synthesis. The libraries included mutations in and around LysU's active-site aimed at increasing the Ap4A synthetase activity, and consensus mutations to compensate for the stability losses associated with the function altering mutations (Table S1). Following 3 rounds of mutagenesis and screening for higher synthetase activity, variant A2 (K178E, L231M, V268T, E362R, E373R, F426Y) was isolated. To abolish the aminoacylation activity, we first tried to truncate the N-terminal tRNA binding domain, but this resulted in an almost complete loss of activity. We thus mutated 3 residues known to mediate tRNA binding (R77A, Q95A, T130A) [43,44]. The new LysU variant, dubbed LysU_Ap4Asynth, exhibited ~2-fold increased Ap4A synthetase activity with no detectable aminoacylation activity (Fig 4A).

This article is protected by copyright. All rights reserved.

LysU_Ap4Asynth was expressed from a pZA plasmid in various *E. coli* strains, thus enabling us to examine the outcome of artificially triggered production of Ap4A. Wild-type LysU, and an inactive variant devoid of both aminoacylation and Ap4A synthesis, were used as controls. *E. coli* K12 cells expressing these 3 different LysU variants exhibited the very same growth rate as wild-type, including under heat-shock and starvation (Fig 4B) despite the fact that the cellular concentrations of Ap4A were up to 4.5-fold higher in the strains over-expressing wild-type LysU and its sub-functionalized variant, LysU_Ap4Asynth (Table 1).

As expected in the *ΔapaH* strain, over-expression of LysU, and especially of LysU_Ap4Asynth, resulted in a longer lag phase in minimal medium (Fig 4C). However, the Ap4A concentrations in the *ΔapaH* cells expressing these LysU variants, or with no LysU over-expression, were all similar. This could be due to the fact that Ap4A concentrations were measured during the exponential phase and not during the lag phase, and also because of biases in the calculated concentrations due to differences in cell morphology.

The above result is meaningful, because removal of ApaH results in a huge increase in Ap4A levels (>300-fold; Table 1) and thus causes a global physiological disturbance. It seems, however, that a mild perturbation at the range expected for a signaling molecule has no effect. Further, in direct competition assay the ratio between cells expressing LysU_Ap4Asynth and cells expressing an inactive LysU variant did not change during growth in LB (Fig 4D) or M9-Glc medium (Fig 4E) at 37 °C for 48 h. Thus, a mild increase in Ap4A levels does not confer any advantage or disadvantage.

Overall, these data suggest that untimely and elevated Ap4A production has no observable physiological effect, unless the accumulating Ap4A is not removed (criterion 7 met). Mild increases, *e.g.* 4-fold, had no observable effect, and particularly not higher resistance to heat-

This article is protected by copyright. All rights reserved.

Accepted Article

stress. If anything, elevated Ap4A levels seem to induce heat sensitivity rather than heat resistance. This result is inconsistent with Ap4A playing a role in specific signaling (criterion 3 not met), but is entirely consistent with Ap4A being a damage metabolite.

Proteomics of *E. coli ΔapaH*

We examined the changes in *E. coli's* proteome in the *apaH* knockout whereby Ap4A levels are ~350-fold elevated. We opted for growth in minimal medium, and during the exponential phase, rather than heat-shock, to examine changes that occur prior to, and not during stress. Additionally, although *ΔapaH* cells did not die at 46 °C, they did not grow and hence limited cell mass. Protein intensities in the Δ*apaH* strain were compared to the parental, wild-type strain. We only considered changes in proteins where ≥2 peptides were consistently identified. Overall, ~2,000 proteins, namely about half of the *E. coli* proteome, were reliably detected in both conditions.

The proteome changes were relatively subtle. Only 9 proteins were identified whose levels decreased by 2-13-fold in *ΔapaH* in at least two independent experiments (Table 3). No up-regulated proteins were observed, not reproducibly and given our analysis criteria.

The proteins listed in Table 3 can be divided into 3 groups: (i) proteins regulated by Zur - the Zn^{2+} DNA-binding transcriptional repressor (YkgM, ZinT, ZnuA); (ii) enzymes belonging to aromatic amino acid biosynthesis pathways (AroF, TyrA, TrpE, TrpA); (iii) proteins that regulate the starvation sensing during stationary phase (RspA, RspB). The last two groups are related because a shortage of aromatic amino acids is known to be a hallmark of starvation [45]. It therefore appears that elevated Ap4A levels result in a lower ability to sense starvation, thus accounting for the slower recovery of Δ*apaH* strain after starvation and

This article is protected by copyright. All rights reserved.

Accepted Article

probably also for the growth arrest at 46 °C. Indeed, we observed no indications for a heat-stress response - most heat-shock proteins and chaperones were reliably detected and showed no changes.

Ap4A and Zn^{2+} homeostasis

A distinct change in response to elevated Ap4A levels was the decrease in expression of 3 out of the 5 operons controlled by the zinc transcriptional factor, Zur. Down-regulation the other two operons was also observed (*pliG* and *znuB,C*), with a milder, ~1.5-fold decrease. The result is in accordance with the affinity of Zur for those operons. The strongest binding was reported to the *ykgM,O* operon and the weakest to *pliG* [46]. The down-regulation of Zur-regulated genes, including the Zn^{2+} importer, suggests that the Δ*apaH* strain has elevated cellular zinc levels, or perhaps that erroneously senses high levels. If the Δ*apaH* strain has increased intracellular zinc concentration, then the *apaH* knockout strain might exhibit some advantage in a Zn^{2+} depleted media. Indeed, while the parental K12 strain showed no growth in minimal medium containing the metal chelator EDTA, the Δ*apaH* strain grew after a lag phase to a final cell density that is similar to that without a chelator (Fig 5). Although EDTA chelates a range of bivalent metals including Mg^{2+} and Ca^{2+}, its affinity towards zinc is $\geq 10^5$-fold higher, and the concentrations of the latter were higher than that of EDTA.

Overall, the proteomics data are consistent with the observed phenotype of the Δ*apaH* strain in relation to its compromised response to starvation. Further, these data do not indicate a linkage between Ap4A and heat-stress. However, we observed a previously unreported linkage between Ap4A and Zn^{2+} homeostasis that may relate to the observation that Ap4A binds Zn^{2+} with high affinity [47]. Although the affinity measurement was later questioned [48], Zn^{2+} is also known to activate the Ap4A synthetase activity of AARS [49]. However, while Ap4A may contribute to zinc storage under some conditions, a specific role for Ap4A

This article is protected by copyright. All rights reserved.

Accepted Article

in sensing Zn^{2+} depletion is unlikely, given that, as discussed in the next section, none of the identified putative Ap4A binders are associated (regulatory, or otherwise) with Zn^{2+} homeostasis.

Identification of Ap4A binding proteins in *E. coli*

If Ap4A is part of a signaling network, this network must involve selective Ap4A binding to at least one protein. Previous attempts to identify Ap4A binders yielded few putative targets including DnaK [20], ClpB [50], GroEL [20] and IMPDH [51]. We attempted to identify Ap4A binding proteins by pull-down with biotin labeled Ap4A. We tested several biotinylated analogs, yet the only one that gave consistent results had the biotin tethered to the N8 of the adenine ring (as opposed to attachment via the ribose or adenine-N6). Owing to the minimal interference of N8 modification, this analog was also the only one that could be enzymatically synthesized from N8-biotinylated ATP using Apa2, the yeast Ap4A phosphorylase, which catalyzes the conversion of adenosine-5'-phosphosulfate (APS) and ATP into Ap4A [52]. Pull-downs were performed in two alternative modes: The lysate was pre-incubated with biotin-Ap4A, and the streptavidin beads were added later; or, with streptavidin beads pre-coated with biotin-Ap4A. In both modes, ATP was present in the binding step to favor selective Ap4A binders. After extensive washing, the remaining, bound proteins were identified by shotgun proteomics. As controls, pull downs were performed with either biotin, or biotin-ATP.

Potential Ap4A binders were identified on the basis of a cumulative score that included 3 criteria: (i) The number of unique peptide fragments that are observed (2 as a minimum); (ii) > 2-fold enrichment in the biotin-Ap4A samples relative to the biotin and biotin-ATP controls; (iii) consistent enrichment in more than one pull-down. The highest scoring proteins are listed in Table 4. A few of these were previously implicated with Ap4A binding (IMPDH,

This article is protected by copyright. All rights reserved.

Accepted Article

DnaK). Interestingly, most of these putative Ap4A binders are regulatory proteins, with particular enrichment of ssDNA binding proteins. However, although all pull-downs were done in the presence of ATP to minimize unspecific binding, nearly all the identified proteins are known ATP binders.

The two proteins showing the highest enrichments in all pull-down experiments were inosine monophosphate dehydrogenase (IMPDH; previously implicated with Ap4A [51]) and a transcriptional regulatory protein, NrdR. These were further characterized to determine if Ap4A binding is biologically relevant.

IMPDH binds Ap4A but with no selectivity over ATP

IMPDH catalyzes the NAD-dependent oxidation of inosine-5'-monophosphate (IMP) to xanthosine 5'-phosphate (XMP) [53]. Bacterial IMPDHs possess an additional domain, a cysthathionine β-synthase (CBS) domain, that acts as transcriptional regulator [54] in maintaining the ATP/GTP pool [55]. Accordingly, the CBS domain binds phosphorylated nucleosides such as ATP or AMP that may comprise allosteric regulators of IMPDH, and also binds ssDNA [56]. Bacterial IMPDHs are divided to two classes: *Class I* comprises enzymes that are allosterically activated by ATP and are permanently octameric; *Class II* enzymes exhibit ordinary kinetics, are tetramers in the apo state, and shift to octamers in the presence of NAD or ATP [57]. *E. coli*'s IMPDH (*ec*IMPDH) belongs to Class II, yet aiming to examine how evolutionary conserved Ap4A binding is, we also tested a IMPDH from *P. aeruginosa* that belongs to Class I.

In agreement with its dominance in pull-downs, purified *ec*IMPDH exhibited tight binding to biotinylated-Ap4A (Fig 6A). Soluble ATP or Ap4A did not inhibit binding, suggesting a large avidity effect (multiple immobilized Ap4A molecules and IMPDH's octameric state). Using radioactively labeled Ap4A and equilibrium dialysis, we confirmed that *ec*IMPDH

This article is protected by copyright. All rights reserved.

Accepted Article

binds soluble Ap4A with 5-fold higher affinity than ATP. This affinity ratio indicates that Ap4A binding is physiologically irrelevant. Cellular ATP concentrations in *E. coli* are in the range of 1-10 mM [58,59] while Ap4A's concentration is in the range of 0.2 µM (Table 1). In fact, ATP dominates (≥ 14-fold molar excess) even at the abnormally high Ap4A concentrations observed in the *apaH* knockout (~70 µM).

Indeed, we could not identify any physiologically relevant modulation of *ec*IMPDH by Ap4A. Neither ATP nor Ap4A influenced the enzymatic activity of ecIMPDH (Fig 6B). Both ligands inhibited the binding of *ec*IMPDH to ssDNA, but in the same manner, and in any case, significant inhibition by Ap4A was only observed at 0.1 mM, *i.e.*, at a physiologically irrelevant range (Fig 6C).

In contrast to the Class II *ec*IMPDH, the Class I IMPDH of *P. aeruginosa* (*pa*IMPDH) is allosterically activated by ATP [60]. We found that Ap4A is a weaker allosterically activator of *pa*IMPDH and competes for the same binding site as ATP (Fig 6D). However, the effect of Ap4A could only be observed at ATP concentrations below 1 mM (Fig 6E and Fig 6F). Further, even at 0.1 mM ATP (10-fold below the minimal reported cellular concentration), the effect of Ap4A was only seen at 10 µM (50-fold above the normal cellular levels).

Overall, our results indicate that although *in vitro* Ap4A binds and modulates IMPDHs belonging to both Class I and II, *in vivo* Ap4A is unlikely to be relevant because its effects are completely masked by ATP. From the point of view IMPDH's physiological role, our results suggest that ATP comprises an inhibitor of ssDNA binding. Thus, ATP is not only an allosteric and oligomeric regulator of IMPDHs [60], but may also affect their function as transcriptional regulators. Specifically, IMPDHs have been suggested to suppress transcription of genes involved in adenylate nucleotide synthesis [56] and our results suggest that ATP binding to the CBS domain of IMPDH may alleviate this suppression.

This article is protected by copyright. All rights reserved.

Accepted Article

NrdR also binds Ap4A as an ATP surrogate

The second-best Ap4A binder identified by our pull-downs was NrdR – a zinc-finger transcriptional regulator that modulates the expression of several operons encoding ribonucleotide reductases (RNRs) according to the abundance of deoxyribonucleoside triphosphates (dNTPs) relative to ribonucleotides (NTPs) [61,62]. NrdR has been reported to bind ATP [62]. We confirmed NrdR's strong affinity to biotinylated Ap4A immobilized onto streptavidin plates, as opposed to no binding of immobilized ATP (Fig 7A). Subsequently, we compared the effect of Ap4A and ATP on NrdR's binding to DNA. NrdR regulates RNRs expression through binding to so-called 'NrdR boxes', 16 bp motifs within RNRs promoters. We used a 237 bp dsDNA stretch that corresponds to *nrdA* promoter region and assayed NrdR's binding as for IMPDH. Although Ap4A showed a slightly stronger inhibitory effect, under our assay conditions, ATP completely inhibited DNA binding at 0.1 mM concentrations (Fig 7B).

Other putative Ap4A binding proteins

The effect of Ap4A on DNA binding was also tested for transcriptional regulators HU and HNS, which were also identified in the pull-downs, but our *in vitro* assays indicated that Ap4A did not modulate DNA binding of these proteins.

DnaK and ClpB are reported Ap4A binders [20,50] and DnaK was also identified in our pull-downs. Both proteins (DnaK, ClpB) are part of a chaperone complex that includes DnaJ and GrpE [63]. We tested the effect of Ap4A on the refolding activity of the DnaK-DnaJ-GrpE-ClpB complex but did not observe a significant effect. Since the DnaK-DnaJ-GrpE complex is also involved in bacteriophage λ DNA replication, we tested the effect of ATP and Ap4A on ssDNA binding. ATP strongly activated DnaK's binding to ssDNA while Ap4A had no effect.

This article is protected by copyright. All rights reserved.

Accepted Article

In conclusion, the pull-down experiments did not identify selective Ap4A binders, let alone proteins where Ap4A binding has potential relevance *in vivo*. As is clear from the detailed analysis of IMPDH and NrdR, Ap4A binds these proteins as an ATP surrogate. Furthermore, although IMPDH and NrdR bind Ap4A at the μM range, and in some *in vitro* assays exhibit higher affinity to Ap4A compared to ATP, a biological relevance is unlikely. Firstly, because the cellular ATP concentrations are normally ≥ 5,000-fold higher compared to Ap4A (1-10 mM *versus* 0.2 μM, respectively). Secondly, none of the genes/proteins that are under regulation of the proteins identified as potential Ap4A binders exhibited changes in expression in the *apaH* knockout. For example, the levels of proteins under NrdR's regulation (NrdA, NrdB, NrdE, NrdI) did not change at elevated Ap4A levels (Table 3). Thus, the effects of Ap4A on NrdR do not seem to differ from those of ATP, certainly not in the concentration range that is physiologically relevant. Conversely, none of the proteins whose expression significantly changes in *apaH* knockout is linked, even indirectly, to the identified Ap4A binders (criterion 4 not met).

Discussion

It is generally easier to prove the existence of a given biological mechanism, or entity, than to prove its absence (which in some cases, would be impossible). Nonetheless, a set of Occam's razor criteria can be applied to distinguish between two alternative hypotheses: a damage metabolite versus a specific signaling role. In the case of Ap4A in *E. coli*, all criteria for damage metabolite were met as opposed to none of those indicating specific signaling. However, it is clear that these results do completely not rule an involvement of Ap4A in signaling. Firstly, our assays were limited to starvation and heat stress, and Ap4A could be involved in signaling other challenges. Secondly, Ap4A could be indirectly involved, for

This article is protected by copyright. All rights reserved.

Accepted Article

example, via the modulation of other alarmones such as ppGpp. Finally, a lack of signaling function in *E. coli* does not exclude the possibility that Ap4A acts as secondary messenger, and especially in mammalian cells [64]. The new tools we have established allow controlled perturbations of cellular Ap4A concentrations. Beyond the routinely applied knockout of Ap4A hydrolase, an Ap4A synthetase is now available that may assist the identification of signaling roles of Ap4A, in *E. coli* or another organism.

Given the complexity of the cellular milieu, we recognize the risk of claiming that we have exhausted the search for function. On the other hand, not every compound in the cell must have function. There exists a Panglossian tendency to assume that "any trait has to have a good use to explain its presence". However, "the default assumption should now be that the products of metabolite damage are merely adventitious, particularly if there is an efficient system to remove them" [31]. As shown here, Ap4A is not only efficiently removed in *E. coli*, but also constitutively – neither the expression nor the enzymatic activity of its Ap4A hydrolase are regulated. Additionally, only massive accumulation of Ap4A such in the case of ApaH knockout induces phenotypic changes. Unlike in the case of alarmone where even 2-fold increase above basal level has effect, slight Ap4A increase or decrease observed with expression of LysU variants, and Apa2, respectively, did not affect cell fitness. Effects of mild Ap4A increase or decrease were not observed even in growth competitions that can detect relatively subtle effects. These results are in clear contrast to what had been observed with other alarmones, most distinctly with ppGpp that bears obvious analogy to Ap4A. Subtle changes in ppGpp levels, in the order of 10-fold, affected growth rate [23]. Over-expression of ppGpp synthase results in severe growth inhibition [27], while strains lacking ppGpp show complex phenotypes, from amino acid auxotrophy to morphological changes [26].

This article is protected by copyright. All rights reserved.

Our results also indicate two potential toxic effects of Ap4A accumulation. Firstly, Ap4A mimics ATP. The pull-down experiments identified known ATP binders. Their characterization indicated that Ap4A can displace ATP and inhibit those proteins. Indeed, enzyme inhibition by mimicry is a common effect of damage metabolites. For example, spontaneously modified products of NADH and NADPH at neutral pH, cannot serve as electron acceptors or donors, but they bind and inhibit dehydrogenases [65]. Secondly, high Ap4A concentrations seem to disrupt Zn^{2+} homeostasis. The proteome analysis revealed that high Ap4A levels inhibit expression of Zn^{2+} importers. Accordingly, the growth advantage of the *ΔapaH* strain in Zn^{2+}-deficient medium suggests that high Ap4A levels lead to increase in Zn^{2+} levels.

In *E. coli*, and as far as we know, in other organisms, Ap4A is not produced by a dedicated enzyme, but rather, it is a side-product of one of the most ancient and essential enzyme classes, AARSs. Although Ap4A is probably present in all organisms, not all aminoacyl-tRNA synthetases produce it, certainly not to the same degree. This observation, and the deleterious effects of accumulating Ap4A, may suggest that, unless beneficial, Ap4A production by AARSs would have been eliminated by evolution. However, whether Ap4A production can be eliminated with no effect on AARS function is unknown. Thus, AARSs could be yet another example, out of many, where the most accessible evolutionary solution was an enzyme that degrades the damage metabolite rather than eliminating its production in the first place.

This article is protected by copyright. All rights reserved.

Accepted Article

Material and methods

Bacterial strains and procedures

The applied *E. coli* strains are listed in Table 1. *E. coli* K12 *ΔapaH* strain was generated by P1 transduction [66] using the *apaH* knockout from Keio collection [67] as a starting point. The strains where the *apaH* gene was replaced with other genes were generated using the λ-red system [68], whereby the kanamycin cassette in *E. coli* K12 *ΔapaH* strain was replaced with the open reading frame of the complementing gene followed by a chloramphenicol cassette.

The open-reading frame (ORF) of the *apa2* gene (Gene ID: 852143) was PCR amplified from the genome of *S. cerevisiae* ATCC 204508/S288c, and cloned into a pZA vector with anhydrous tetracycline inducible promoter [69]. The list of primers used for cloning is provided as Table S2. The inactive variant Apa2-H161A was generated by site directed mutagenesis [70]. Plasmids were transformed to *E. coli* K12 or its *ΔapaH* strain, using ampicillin (100 µg/ml) as a selection marker.

Growth experiments were done in LB, or in M9 medium plus 0.4 % glucose (M9-Glc) without presence of antibiotics. A pre-culture in LB, or M9, with antibiotics (2 ml; grown for 24 h), was diluted to OD_{600nm} = 0.2, and 3 µl inoculates were transfer to 150 µl of LB, or M9-Glc, in 96-well microtiter plates. Growth was subsequently followed in a plate reader (BIO-TEK, Synergy HT), at 37 °C with shaking (for 30 s with 5 min intervals) while monitoring OD_{600nm}. Growth at elevated temperature was followed in LB. Inoculating an LB culture as above, and growing in a plate reader at 46 °C. The inoculated culture was overlaid with 100 µl of mineral oil to prevent evaporation. Growth of strain carrying pZA plasmids (encoding ApaH, Apa2 or LysU variants) was done as above, except that ampicillin, and anhydrous tetracycline (AHT; 200 ng/ml) as inducer, were added.

This article is protected by copyright. All rights reserved.

Accepted Article

Growth competitions

We used two platform strains, both containing *E. coli*'s original ApaH gene: unmodified *E. coli* K12, or *E. coli* K12 *ΔapaH::apaH-CAP* that contains the original *apaH* gene alongside a chloramphenicol (CAP) cassette used as a marker. *E. coli* K12 that carried pZA_Apa2 H161A plasmid (inactive Apa2) served as the reference strain. The competing strains were based on *E. coli* K12 *ΔapaH::apaH-CAP*. They carried either pZA_Apa2 H161A plasmid (inactive apa2) or pZA_Apa2 (active apa2). These strains were grown separately in LB *plus* Amp (100 µg/ml) until OD_{600nm} ~ 1. They were then mixed at a 1:1 ratio. An aliquot of this mix was immediately diluted and plated in parallel on LB agar *plus* Amp, and LB agar *plus* Amp *plus* CAP, to measure the initial cell counts of each strain. Another aliquot of the starting mix was diluted 1000-fold in 8 ml of LB *plus* Amp *plus* AHT (100 ng/ml), and in 8 ml of M9-Glc *plus* Amp *plus* AHT (100 ng/ml). After 24 h growth at 37 °C (200 rpm, 50 ml falcon tubes), the resulting cultures were plated in parallel on selective LB agar to measure the cell counts of the two competing strains. An aliquot of 24 h culture was diluted 1000-fold in the fresh medium (serial passage) and after 24 h of growth at 37 °C the cultures were plated again on selective agar to measure the cell counts.

The control competition was of [*E. coli* K12 pZA_Apa2 H161A] versus [*E. coli* K12 *ΔapaH::apaH-CAP* pZA_Apa2 H161A] thus determining the effect of chloramphenicol cassette at wild-type like Ap4A levels (inactive Apa2, in both strains). Subsequently, [*E. coli* K12 pZA_Apa2 H161A] was competed *versus* [*E. coli* K12 *ΔapaH::apaH-CAP* pZA_Apa2] to measure the fitness effects associated with decreased Ap4A level.

The same procedure was used for the fitness assay with the increased levels of Ap4A. *E. coli* K12 carrying pZA_InT plasmid (inactive variant of LysU) was competing against *E. coli* K12 *ΔapaH::apaH-CAP* pZA_InT and *E. coli* K12 *ΔapaH::apaH-CAP* pZA_Ap4Asynth.

This article is protected by copyright. All rights reserved.

Accepted Article

Data are presented as percentage of selected strain (number of colonies on LB agar + Amp + CAP) versus total cell number (number of colonies on LB agar + Amp) with standard deviation from 3 biological replicas.

ApaH cloning, purification, activity and thermal denaturation assay

The ORF of *apaH* gene (Gene ID: 944770) was PCR amplified from the genome of *E. coli* K12 and cloned into a pET-21a vector with a C-terminal 6-His tag. A synthetic gene encoding the designed ApaH_D7 (D7 design contains following mutations: I17Q, H21D, E24N, T26D, G28K, D47K, Y51F, F74A, S78R, K114R, T124A, Q130E, D138E, S147N, F150W, D153E, H162R, R168T, G171D, N189D, Q191R, Y195K, S196C, P206E, G215S, A218S, E219K, S222N, E238P) was cloned in pET21a vector with the same tag. The H120A and H227A mutants of ApaH_D7 were generated by site directed mutagenesis. The recombinant plasmids were transformed into *E. coli* BL21 (DE3) and cultured in 100 ml LB medium. Protein expression was induced with 1 mM IPTG at $OD_{600nm} \approx 0.6$. After being cultured for another 6 h at 37 °C, cells were harvested, collected by centrifugation, and resuspended in 5 mL of lysis buffer (50 mM HEPES, pH 7.8, and 150 mM KCl, 15 mM imidazole). After sonication and removal of pellet, the proteins in the supernatant were loaded on a Ni-NTA column that was pre-equilibrated with the binding buffer (50 mM HEPES, pH 7.8, and 150 mM KCl). The ApaH variants were eluted with 200 mM imidazole, elution fractions were pulled, the buffer was exchanged to 50 mM HEPES, pH 7.8, 150 mM KCl, 7 mM $MgCl_2$, and the proteins concentrated to 0.15 mg/ml, 9 mg/ml, 7.8 mg/ml, 4.1 mg/ml wild type ApaH, ApaH_D7, ApaH_D7 H120A and ApaH_D7 H227A, respectively. Protein purity was assessed by electrophoresis and the samples were stored at -20 °C.

This article is protected by copyright. All rights reserved.

The thermal stability of ApaH variants was measured following heat-induced unfolding. Solutions of 15 μM enzyme containing 5× SYPRO Orange dye (Invitrogen) were heated from 4 to 99 °C in a 7500 Fast Real-Time PCR system (Applied Biosystems) and unfolding was followed by measuring the change in fluorescence excitation, 488 nm; emission, 570 nm). Measurements were conducted in duplicates and the midpoint of denaturation (T_M) was determined as the maximum of the first derivative for each temperature.

Ap4A hydrolase activity was assayed using 0.15 μM (wild type, and stabilized variant) or 12 μM (D7 variants H120A and H227A) enzyme, 1 mM Ap4A, in 50 mM HEPES, pH 7.8, and 150 mM KCl, 7 mM $MgCl_2$. Aliquots of the reaction mixtures (1.5 μl) were taken at after 5, 10 and 60 min, and analyzed by thin-layer chromatography (TLC) using silica-gel-60 plates with fluorescent indicator (Merck; catalog no. 5554). The mobile phase comprised a mixture of isopropanol:2,4-dioxane:water:25 % ammonia solution at a ratio of 2:4:4:3 [71]. The plates were dried and visualized by UV light. Samples were run in duplicates and the UV images were analyzed by IMAGEJ.

Cloning, expression and purification of Apa2

Full-length *apa2* gene (Gene ID: 852143) was PCR amplified from the genome of *S. cerevisiae* ATCC 204508/S288c and cloned into a pET- 21a vector, with an C-terminal hexahistidine tag. The recombinant plasmid was transformed into *E. coli* BL21 (DE3) cultured in 100 ml LB medium. The expression of the proteins was induced with 1 mM IPTG when OD_{600nm} reached 0.6. After being cultured for another 16 h at 20 °C, cells were harvested and collected by centrifugation at 4000 g for 15 min, and resuspended in 5 mL of lysis buffer (20 mM TRIS, pH 7.8, and 150 mM KCl, 15 mM imidazole). The purification procedure is the same as described above for ApaH. Purified protein (5.7 mg/ml) in 20 mM TRIS, pH 7.8, and 150 mM KCl buffer was stored at -20 °C for further use.

This article is protected by copyright. All rights reserved.

Accepted Article

LysU engineering and characterization

The ORF of *lysU* gene (Gene ID: 948645) was PCR amplified from the genome of *E. coli* and cloned into pET-21a, with an C-terminal 6-His tag. The *lysU* gene library was generated using the ISOR method [72], including functional mutations in aminoacylation domain and consensus mutations derived from a sequence alignment (the list of library mutation primers is in Table S2). The assembly PCR was optimized to yield ~2.5 mutations per gene, thus resulting in ~ 50 % of active clones.

The library was cloned in pET-21a and transformed into *E. coli* BL21 (DE3) cells. Single colonies were inoculated in 500 µl LB media and grown overnight at 37 °C in deep-well plates. This preculture (8 µl) was used to inoculate 800 µl of 2YT medium. After 2.5 h of growth at 37 °C with shaking, expression was induced with 1 mM IPTG, and growth was continued for 6 h at 37 °C. The cell pellet was lysed in 20 mM TRIS pH 7.5, 150 mM KCl, 7 mM $MgCl_2$ with bensonase (1 U/µl), lysozyme (0.3 mg/ml) and protease inhibitor (Sigma Aldrich, S8830). For assaying Ap4A synthesis, 5 µl of clarified lysate was added to 45 µl of reaction buffer (20 mM TRIS pH 7.5, 150 mM KCl, 7 mM $MgCl_2$) plus mixture with 1 mM ATP. The reaction was incubated for 1 h at 37 °C and stopped by heating (5 min at 65 °C). The unreacted ATP was hydrolyzed by calf intestine phosphatase (4 U) for 3 h min at 37 °C, and the phosphatase was inactivated by heating at 85 °C for 5 min. A 10 µl aliquot of the inactivated reaction mix was added to 9.75 µl aliquot of the luciferase ATP determination kit (LBR-T010, Proteinkinase.de) plus recombinant human Ap4A hydrolase in order to hydrolyze the synthesized Ap4A to AMP and ATP (0.25 µl of 1 mg/ml; the enzyme was cloned in pET-21a with C-terminal His tag and purified as Apa2). The assay was calibrated such that the amount of ATP generated by Ap4A hydrolysis was proportional to the luminescence signal. The first-round variants that showed higher activity that wild-type LysU were reshuffled to generate the second library. The variants with the highest Ap4A synthetase

This article is protected by copyright. All rights reserved.

Accepted Article

activity were characterized as described below. The mutations in the tRNA binding domain (R77A, Q95A, T130A) were introduced by site directed mutagenesis protocol [70].

The engineered LysU variants were expressed in *E. coli* BL21 (DE3) cells cultured in 100 ml LB. Expression was induced with IPTG, and growth was continued for 6 hr as above. The purification procedure was the same as for Apa2 described above.

Ap4A synthesis and aminoacylation assay

Ap4A synthesis was assayed by the luminescence assay or by HPLC. The reaction mixture contains 0.05 mg/ml LysU variants, 2.5 mM ATP and 0.2 mM lysine, in 20 mM TRIS pH 7.5, 150 mM KCl, 7 mM $MgCl_2$. At different time points, aliquots of 10 µl were added to acetonitrile (10 µl), diluted 5 times in water, filtered through 0.2-µm filters (0.22 µm, Millex-GV 4 mm PVDF, Merck-Millipore) and loaded on ion-exchange HPLC column (SAX-NP5, 50x4.6 mm). The mobile phase comprised 10 mM TRIS pH 7.2, and elution with a gradient of NaCl (from 0 to 0.5 M NaCl in 10 minutes). The faction of ATP and Ap4A was determined by relative peak intensities (OD_{260nm}).

Aminoacylation was assayed in 50 µl reactions, contacting 0.1 mg/ml LysU variants, 2 mM ATP, 0.2 mM lysine (spiked with 1 µCi of ^3H labeled lysine, Perkin Elmer NET376250UC) and 10 µM tRNALys, in 20 mM TRIS pH 7.5, 150 mM KCl, 7 mM $MgCl_2$, incubated at 37 °C for 2-12 h. Reactions were stopped by addition of 100 µl of salmon sperm DNA (1 mg/ml, in sodium acetate pH 3.0) followed by 150 µl of 20 % TCA. The pellet was isolated and washed 4 times with 5 % TCA containing 0.2 mM cold lysine by centrifugation. The last washing was with 96 % ethanol, and the precipitate was then dried and dissolved in 75 µl of 0.1 M NaOH. The resuspended samples were added to 3 ml of liquid scintillation cocktail (Ultima Gold; Perkin Elmer) and analyzed in a liquid scintillation analyzer (Packard TRE-CARB 2100TR).

This article is protected by copyright. All rights reserved.

Accepted Article

Determination of cellular Ap4A concentrations

Extract preparation

E. coli K12 wild type and *ΔapaH* cultures were grown in M9-Glc for 24 h , and used to inoculate a fresh 10 ml culture of M9-Glc (at 100 dilution). The cultures were grown with shaking at 37 °C and cells were pelleted by 3 min centrifugation at 10000 g, at $OD_{600nm} \approx 0.3$ (exponential). The cell pellets were frozen in liquid nitrogen and analyzed by MS. The samples were extracted with methanol-acetonitrile-water [40:40:20] with 0.1 N formic acid. The internal standard mix (15 µL) was added to the extracts, and the obtained mixtures were concentrated in speedvac to eliminate extraction solution, and then lyophilized till dryness. Before LC-MS analysis the obtained residues were re-dissolved in 50 µl of starting eluent (70 % A/30 % B), and filtered through 0.2-µm filters (0.22 µm, Millex-GV 4 mm PVDF, Merck-Millipore) to remove insoluble material.

Preparation of internal standard mix

$^{13}C_{10}$-ATP (2 mM, Sigma Aldrich cat. number 710695) was reacted with 0.25 mM lysine and LysU enzyme (0.1 mg/ml) to produce $^{13}C_{20}$-Ap_4A. The reaction progress was followed by TLC (method described above), at 10 % of conversion the enzyme was eliminated by addition of acetonitrile (1:1 v/v) to prevent further reaction progress. Precipitated enzyme was removed by centrifugation, solution diluted 2-fold in water and filtered through 0.2-µm filters. To prepare internal standard mix stock, the reaction mixture was diluted in water providing 5 µM concentration of $^{13}C_{20}$-Ap_4A and 45 µM of $^{13}C_{10}$-ATP.

LCMS analysis

The LC-MS/MS instrument consisted of Acquity I-class UPLC system (Waters) and Xevo TQ-S triple quadrupole mass spectrometer (Waters) equipped with an electrospray ion source and operated in positive ion mode was used for analysis of nucleoside phosphates. MassLynx

This article is protected by copyright. All rights reserved.

Accepted Article

and TargetLynx software (v.4.1, Waters) were applied for the acquisition and analysis of data. The analysis was done on a 50 x 2-mm i.d., 3-µm 100 Å Luna-NH2 column equipped with 4.0 x 2.0 security guard amine cartridge (both Phenomenex) with mobile phases A (10 mM ammonium formate, pH 5.0 adjusted with 10 % acetic acid, followed by addition of 40 mL of acetonitrile) and B (1 mM ammonium formate, pH 10.6 adjusted with 29 % ammonia, followed by addition of 17 mL of acetonitrile) at a flow rate of 0.3 ml/min and column temperature 25°C. A 10-minute gradient was as follows: linear increase from 30 to 70 % B during 4 minutes, then increase to 90 % in 0.5 minute, followed by return to 30 % B in the next 0.5 minute, and equilibration for 5 minutes. Samples kept at 4°C were automatically injected in a volume of 5 µl.

For mass spectrometry argon was used as the collision gas with flow 0.10 ml/min. The capillary voltage was set to 2.50 kV, source temperature - 150°C, desolvation temperature - 600°C, desolvation gas flow - 800 L/h. Analytes were detected using multiple reaction monitoring (MRM) applying following parameters: Ap4A (retention time 3,57 min; transition 837.1>136.2 (cone 14 V, CE 35 eV); transition 837.1>348.2 (cone 14 V, CE 26 eV)), $^{13}C_{20}$-Ap4A (retention time 3,57 min; transition 857.1>141.1 (cone 14 V, CE 35 eV); transition 857.1>358.1 (cone 14 V, CE 26 eV)), $^{13}C_{10}$-ATP (retention time 3,90 min; transition 518.0>141.1 (cone 14 V, CE 35 eV); transition 508.0>358.1 (cone 14 V, CE 18 eV)).

Cellular concentration was determined in two ways: based on the dry weight of the extracted cells and OD_{600nm}. The total intracellular volume: the dry weight of the extracted cells (measured using cultures that are treated identically to those used for metabolite extraction) multiplied by the ratio of aqueous volume to cellular dry weight. The ratio of aqueous volume to cellular dry weight is 0.0023 liter g/1 for *E. coli* [73]. The total intracellular volume calculated on the basis of the OD_{600nm}: total number of cells (OD_{600nm} = 1 corresponds to 10^9 cells/ml) multiplied by the single cell volume (1 μm^3 [74]). The measured concentration was

This article is protected by copyright. All rights reserved.

Accepted Article

multiplied with dilution factor (sample volume/total cellular volume) to determine intracellular concentration of Ap4A. Concentrations calculated by both methods were similar.

Synthesis of biotin labeled Ap4A

Synthesis of 8-[(6-amino)-hexyl]-amino-Ap4A-biotin

The reaction mixture contained 0.25 mM 8-[(6-amino)-hexyl]-amino-ATP-biotin (NU-807-BIO, Jena Bioscience), 0.5 mM adenosine-phosphosulfate (APS) and 0.25 mg/ml Apa2, in a reaction buffer of 50 mM HEPES, pH 7.8,150 mM NaCl and 1 mM $MgCl_2$. The reaction was analyzed by HPLC (ion-exchange, as above). Apa2 was removed from reaction mixture by centrifugation through 10 kDa cut-off spin column (Millipore) and samples were stored at -20 °C. Using the same protocol, ^{3}H-labeled Ap4A was synthesized from ^{3}H-ATP (NET420250UC, Perkin Elmer).

Synthesis of PEG_3-biotin Ap4A

In a round bottom vial, 0.012 mmol (10.0 mg) of Ap4A (Sigma) and 0.014 mmol (2.33 mg) of carboxydiimidazole (CDI) were added in 70 µl of water. The vial was vibrated for 30 minutes, after which PEG_3-Biotin (Pirece) was added. The vial was vibrated overnight at room temperature and product formation was monitored by TLC (dioxane/isopropyl alcohol/ 25% NH_4OH/ 6 mM EDTA; 4:2:3:4). Water was removed by lyophilisation and the crude product was obtain as waxy white solid. ^{1}H-NMR and ^{31}P-NMR were recorded in D_2O at ambient temperature (20°C) operating at 300 MHz and 121.5 Mhz respectively.

^{1}H-NMR (300 MHz, D_2O) δ 8.34 (2H, s), 8.06 (2H, s), 5.96 (2H, d), 4.68 (2H, t), 4,51(3H, m), 4,23-4,00 (7H, m), 3.60-3.40(12H,m), 3.20 (2H, m), 3.10 (1H,m), 3.01 (2H, t), 2.80 (1H, m), 2.58 (1H, m), 2,11(2H, m), 1.59-1.1 (6H, m). To be noted is the upfield shift of the

This article is protected by copyright. All rights reserved.

Accepted Article

triplet due to the methylene group (3.01 ppm, -CH_2-CH_2-NH-P(O)(OR_2)-) in alpha position respect to the terminal amine of the PEG_3-Biotin chain (2.68 ppm, -CH_2-CH_2-NH_2). ^{31}P-NMR (121.5 MHz, D_2O) δ -10.30, -22.13.

It appears, however, that the p-NH- bond was unstable, thus making this mode of coupling inapplicable for pull-downs.

Proteomics and pull-down experiments

Proteomics: The culture was prepared in the same way as described above for metabolomic analysis. The cell pellets were frozen in liquid nitrogen and analyzed by MS.

Pull-down experiments: *E. coli* K12 MG1655 cells were cultured in 10 ml of LB medium and pelleted at $OD_{600} \approx 0.5$. Cell pellets were isolated by centrifugation, washed and resuspended in 50 mM HEPES, pH 7.8,150 mM NaCl and 1 mM $MgCl_2$. Cells were disrupted by sonication. The total protein concentration was measured by BCA kit (23227, ThermoScientific) and all lysates were all diluted to 2 mg protein/ml. Pull-downs were performed with either pre-coated magnetic beads (Merck Millipore, LSKMAGT10), or by pre-incubation with biotinylated ligands. Overall, 3 parallel pull-down experiments were performed. Experiment #1 included the following steps: (*1*) The rinsed beads (1 mg) were incubated with 100 µl of 20 µM biotin, bioATP, or bioAp4A, for 1 h at 4 °C; (*2*) Unbound ligands were removed by rinsing with HEPES buffer (7x250 µl); (*3*) 50 µl of *E. coli* lysate and 50 µM ATP were incubated with biotinylated beads for 1.5 h at 4 °C; (*4*) Unbound proteins were removed by rinsing with HEPES buffer (7x250 µl) and beads were analyzed by MS. Experiment #2 included the following steps: (*1*) 25 µM biotin, bioATP or bioAp4A, were incubated with *E. coli* lysate *plus* 50 µM ATP (100 µl total volume) for 1 h at 4 °C; (*2*) Rinsed beads (1 mg) were added to the above mixture and incubated for an hour at 4 °C; (*3*) Unbound proteins were rinsed by washing with HEPES buffer (7x250 µl) and beads were

This article is protected by copyright. All rights reserved.

Accepted Article

analyzed by MS. Experiment #3 included the following steps: (*1*) Beads (4 mg) were incubated with 400 µl of 25 µM bioAp4A for 1 h at 4 °C; (*2*) Unbound ligand was removed by rinsing with HEPES buffer (7x250 µl); (*3*) BioAp4A beads were incubated with 200 µl of *E. coli* lysate *plus* 50 µM ATP for 1.5 h at 4 °C; (*4*) Unbound proteins were removed by rinsing with HEPES buffer (7x250 µl), and in the last rinse, the beads were split into 4 aliquots (4x100 µl) and buffer was removed; (*5*) Proteins bound to BioAp4A beads were eluted with 100 µl of HEPES buffer, 10 µM, 50 µM, or 100 µM Ap4A solution, and analyzed by MS.

For the MS analysis, samples were subjected to in-solution, on-bead, tryptic digestion. Proteins were first reduced by incubation with dithiothreitol for 30 min at 60°C, and alkylated with 10 mM iodoacetamide in the dark for 30 min at 21 °C. Proteins were then subjected to digestion with trypsin (Promega; Madison, WI, USA) for 16 h at 37°C. The digestions were stopped by trifluroacetic acid (1%). Following digestion, peptides were desalted using solid-phase extraction columns (Oasis HLB, Waters, Milford, MA, USA). The samples were stored in -80˚C until further analysis. For lysate analysis, samples were subjected to in-solution tryptic digestion using a modified Filter Aided Sample Preparation protocol (FASP). Sodium dodecyl sulfate buffer (SDT) included: 4 % (w/v) SDS, 100 mM TRIS pH 7.6, 0.1 M DTT. Urea buffer (UB): 8 M urea (Sigma, U5128) in 0.1 M TRIS pH 8.0 and 50 mM Ammonium Bicarbonate. Cells were dissolved in 100 µL SDT buffer and lysed for 3 min at 95 °C. Then spin down at 16,000 RCF for 10 min. 100 µg were mixed with 200 µL UB and loaded onto 30 kDa molecular weight cutoff filters and spin down. 200 µl of UB were added to the filter unit and centrifuge at 14,000 x g for 40 min. Alkylation using 100 µl IAA, 2 washed with Ammonium Bicarbonate. Trypsin was then added and samples incubated at 37 °C overnight. Additional amount of trypsin was added and incubated for 4 hours at 37 °C. Digested

This article is protected by copyright. All rights reserved.

Accepted Article

proteins were then spun down to a clean collecting tube, 50 µl NaCl 0.5 M was added and spin down, acidified with trifloroacetic acid, desalted using HBL Oasis, Speed vac to dry and stored in -80°C until analysis.

Liquid chromatography

ULC/MS grade solvents were used for all chromatographic steps. Each sample was loaded using split-less nano-Ultra Performance Liquid Chromatography (10 kpsi nanoAcquity; Waters, Milford, MA, USA). The mobile phase was: A) H_2O + 0.1 % formic acid and B) acetonitrile + 0.1 % formic acid. Desalting of the samples was performed online using a reversed-phase C18 trapping column (180 µm internal diameter, 20 mm length, 5 µm particle size; Waters). The peptides were then separated using a T3 HSS nano-column (75 µm internal diameter, 250 mm length, 1.8 µm particle size; Waters) at 0.35 µL/min. Peptides (proteomics analysis) were eluted from the column into the mass spectrometer using the following gradient: 4 % to 20 % B in 155 min, 20 % to 90 % B in 5 min, maintained at 95 % for 5 min and then back to initial conditions.

Peptides (pull-down analysis) were eluted from the column into the mass spectrometer using the following gradient: 4 % to 35 % B in 105 min, 35 % to 90 % B in 5 min, maintained at 95 % for 5 min and then back to initial conditions.

Mass Spectrometry

The nanoUPLC was coupled online through a nanoESI emitter (10 µm tip; New Objective; Woburn, MA, USA) to a quadrupole orbitrap mass spectrometer (Q Exactive HF or Q Exactive Plus, Thermo Scientific) using a FlexIon nanospray apparatus (Proxeon).

Data was acquired in DDA mode, using a Top20 method. For Q Exactive HF analysis, MS1 resolution was set to 60,000 (at 400 m/z) and maximum injection time was set to 20 msec. MS2 resolution was set to 15,000 and maximum injection time of 60 msec. For Q Exactive

This article is protected by copyright. All rights reserved.

Accepted Article

Plus analysis, MS1 resolution was set to 70,000 (at 400 m/z) and maximum injection time was set to 120 msec. MS2 resolution was set to 35,000 and maximum injection time of 60 msec.

Data processing and analysis

Raw data was imported into the Expressionist® software (Genedata) and processed as described here [75]. The software was used for retention time alignment and peak detection of precursor peptides. A master peak list was generated from all MS/MS events and sent for database searching using Mascot v2.5 (Matrix Sciences). For proteomics lysate analysis MS/MS spectra was also searched using MSGF+ (Integrative Omics, https://omics.pnl.gov/software/ms-gf). Data was searched against the *E. coli* K12 protein sequences as downloaded from UniprotKB (http://www.uniprot.org/), and appended with 125 common laboratory contaminant proteins. Fixed modification was set to carbamidomethylation of cysteines and variable modifications were set to oxidation of methionines and deamidation of N or Q. Search results were then filtered using the PeptideProphet [76] algorithm to achieve maximum false discovery rate of 1% at the protein level. Peptide identifications were imported back to Expressions to annotate identified peaks. Quantification of proteins from the peptide data was performed using an in-house script [75].

For lysate analysis protein intensity was normalized based on the total ion current. For pull-down experiments the data was not normalized. Protein abundance was obtained by summing the three most intense, unique peptides per protein. A Student's t-Test, after logarithmic transformation, was used to identify significant differences across the biological replica. Fold changes were calculated based on the ratio of arithmetic means of the case versus control samples.

This article is protected by copyright. All rights reserved.

Accepted Article

Purification and characterization of IMPDHs and NrdR

Full-length *guaB* (Gene ID: 946985) and *nrdR* (Gene ID: 947437) genes were PCR amplified from the genome of *E. coli* and *guaB* gene (Gene ID: 880535) from *P. aeruginosa*. Cloned into a pET-21a vector, with an C-terminal hexahistidine tag. The expression and purification procedure for IMPDHs was the same as for ApaH, while NrdR expression was for 16 h at 16 °C after IPTG induction and purification process the same as described above for Apa2.

IMPDHs (11 mg/ml) were stored in 50 mM HEPES pH 7.8, 150 mM KCl and 7 mM $MgCl_2$ buffer and NrdR (8.9 mg/ml) in 50 mM TRIS pH 8.3, 300 mM NaCl, 5 mM DTT, 100 µM $ZnCl_2$, 20 % glycerol buffer. Proteins were stored at – 20 °C.

For assaying IMPDH's activity 2 µM enzyme was incubated with 1 mM NAD and 2 mM inosine monophosphate (IMP) in reaction buffer of 50 mM HEPES pH 7.8, 150 mM KCl and 7 mM $MgCl_2$. The reaction was monitored by increase in absorbance at 340 nm (Synergy HT, BIO-TEK) in 96-well plates (655801, Greiner Bio-one).

ELISA assays

Binding to DNA was performed by an ELISA-like assay. The promoter region of *gsk* (Gene ID: 946584) and *nrdA* (Gene ID: 946612) genes were amplified from *E. coli* genome using specific primers, followed by a second PCR using a forward biotinylated primer (Table S1). The PCR products were purified, and the DNA concentration was determined by measuring A_{260nm} (NanoDrop 2000, ThermoScientific). Streptavidin-coated plates (StreptaWell, Roche) were incubated for 30 min with 100 µl solutions of either biotin, biotinylated ATP or biotinylated Ap4A (at 2 µM), or biotinylated dsDNA (3 ng/µl). The wells were washed (50 mM HEPES pH 7.8, 150 mM KCl, 7 mM $MgCl_2$), and the ones coated with dsDNA were treated with 0.125 M NaOH (3 x 100 µl) to generate ssDNA [77]. After further washing, the wells were blocked with 1 % BSA. Coated wells were incubated for 1 h with 5 µM

This article is protected by copyright. All rights reserved.

Accepted Article

*ec*IMPDH, *pa*IMPDH, or NrdR in 50 mM HEPES pH 7.8, 150 mM KCl, 7 mM $MgCl_2$, plus various concentrations of ATP and Ap4A as specified. The unbound proteins were washed, and 100 µl 1 µg/ml HRP labeled mouse antiHis-antibody (200 µg/ml, Santa Cruz Biotechnology) was added. Following 1 h incubation, the wells were washed, the substrate was added 3,3',5,5'-tetramethybenzidine (TMB; ES001, Millipore), and OD_{650nm} was monitored .The results are presented as the rate of increase in OD_{650nm}.

Acknowledgments

We thank Prof. Pierre Goloubinoff for materials and assistance with the experimental setup for DnaK chaperone activity. The authors thank Prof. Gad Asher, Dr. Liam Longo and Dr. Miriam Kaltenbach for their comments on the manuscript and Nina Velimirovic for the graphical abstract design. We thank Profs. Ehud Razin and Hovav Nechushtan for discussions and for providing protocols and guidance. We are grateful to Prof. Michael Cashel whose criticism and the discussions following it have been highly constructive and valuable. We gratefully acknowledge financial support from the Rothschild Caesarea Foundation. D.D. acknowledge the Koshland Foundation and McDonald-Leapman grant for financial support. D.S.T. is the Nella and Leon Benoziyo Professor of Biochemistry.

Competing financial interests

The authors declare no competing financial interests.

Author contributions

D.D. and D.S.T. conceived the project, designed the experiments, analyzed the data, and wrote the paper. Y.L. and A.S. performed proteomics, A.B. performed metabolomics analysis and L.F. synthesized PEG_3-biotin labeled Ap4A.

This article is protected by copyright. All rights reserved.

Accepted Article

Accepted Article

References

1. Stephens JC, Artz SW & Ames BN (1975) Guanosine 5'-diphosphate 3'-diphosphate (ppGpp): positive effector for histidine operon transcription and general signal for amino-acid deficiency. *Proc Natl Acad Sci* 72, 4389–4393.
2. Gomelsky M (2011) cAMP, c-di-GMP, c-di-AMP and now cGMP: Bacteria use them all! *Mol Microbiol* 79, 562–565.
3. Ying W (2008) NAD + /NADH and NADP + /NADPH in cellular functions and cell death: regulation and biological consequences. *Antioxid Redox Signal* 10, 179–206.
4. Huang L, Khusnutdinova A, Nocek B, Brown G, Xu X, Cui H, Petit P, Flick R, Zallot R, Balmant K, Ziemak MJ, Shanklin J, de Crécy-Lagard V, Fiehn O, Gregory JF, Joachimiak A, Savchenko A, Yakunin AF & Hanson AD (2016) A family of metal-dependent phosphatases implicated in metabolite damage-control. *Nat Chem Biol* 12, 621–7.
5. Hanson AD, Henry CS, Fiehn O & de Crécy-Lagard V (2016) Metabolite damage and metabolite damage control in plants. *Annu Rev Plant Biol* 67, 131–52.
6. Marbaix AY, Noël G, Detroux AM, Vertommen D, Van Schaftingen E & Linster CL (2011) Extremely conserved ATP- or ADP-dependent enzymatic system for nicotinamide nucleotide repair. *J Biol Chem* 286, 41246–41252.
7. Rosenberg SM, Shee C, Frisch RL & Hastings PJ (2012) Stress-induced mutation via DNA breaks in *Escherichia coli*: A molecular mechanism with implications for evolution and medicine. *Bioessays* 34, 885–892.
8. MacLean RC, Torres-Barcelo C & Moxon R (2013) Evaluating evolutionary models of stress-induced mutagenesis in bacteria. *Nat Rev Genet* 14, 221–227.

This article is protected by copyright. All rights reserved.

9. Randerath K, Janeway CM, Stephenson ML & Zamecnik PC (1966) Isolation and characterization of dinucleoside tetra- and tri-phosphates formed in the presence of lysyl-tRNA synthetase. *Biochem Biophys Res Commun* 24, 98–105.

10. Brevet A, Chen J, Lévêque F, Plateau P & Blanquet S (1989) *In vivo* synthesis of adenylated bis (5' -nucleosidyl) tetraphosphates (Ap4N) by *Escherichia coli* aminoacyl-tRNA synthetases. *Proc Natl Acad Sci USA* 86, 8275–8279.

11. Guo RT, Chong YE, Guo M & Yang X-L (2009) Crystal structures and biochemical analyses suggest a unique mechanism and role for human glycyl-tRNA synthetase in Ap4A homeostasis. *J Biol Chem* 284, 28968–28976.

12. Ogilvie A (1981) Determination of diadenosine tetraphosphate (Ap4A) levels in subpicomole quantities by a phosphodiesterase luciferin--luciferase coupled assay: application as a specific assay for diadenosine tetraphosphatase. *Anal Biochem* 115, 302–7.

13. Farr SB, Arnosti DN, Chamberlin MJ & Ames BN (1989) An apaH mutation causes AppppA to accumulate and affects motility and catabolite repression in *Escherichia coli*. *Proc Natl Acad Sci USA* 86, 5010–4.

14. Lee PC, Bochner BR & Ames BN (1983) AppppA, heat-shock stress, and cell oxidation. *Proc Natl Acad Sci USA* 80, 7496–7500.

15. Bochner BR, Lee PC, Wilson SW, Cutler CW & Ames BN (1984) AppppA and related adenylylated nucleotides are synthesized as a consequence of oxidation stress. *Cell* 37, 225–232.

16. Kimura Y, Tanaka C, Sasaki K & Masashi S (2017) High concentrations of intracellular Ap4A and/or Ap5A in developing *Myxococcus xanthus* cells inhibit sporulation. *Microbiology* 163, 86-93.

This article is protected by copyright. All rights reserved.

Accepted Article

Accepted Article

17. Baker JC & Jacobson MK (1986) Alteration of adenyl dinucleotide metabolism by environmental stress. *Proc Natl Acad Sci USA* 83, 2350–2352.

18. Nishimura A, Moriya S & Ukai H (1997) Diadenosine 5′, 5‴-P1, P4-tetraphosphate (Ap4A) controls the timing of cell division in *Escherichia coli*. *Genes to Cells* 2, 401–413.

19. Pintor J, Peral A, Hoyle CH V, Redick C, Douglass J, Sims I & Yerxa B (2002) Effects of diadenosine polyphosphates on tear secretion in New Zealand white rabbits. *J Pharmacol Exp Ther* 300, 291–297.

20. Johnstone DB & Farr SB (1991) AppppA binds to several proteins in *Escherichia coli*, including the heat shock and oxidative stress proteins DnaK, GroEL, E89, C45 and C40. *EMBO J* 10, 3897–3904.

21. Al Mamun AAM, Lombardo M-J, Shee C, Lisewski AM, Gonzalez C, Lin D, Nehring RB, Saint-Ruf C, Gibson JL, Frisch RL, Lichtarge O, Hastings PJ & Rosenberg SM (2012) Identity and function of a large gene network underlying mutagenic repair of DNA breaks. *Science (80-)* 338, 1344–1348.

22. Hansen S, Lewis K & Vulic M (2008) Role of global regulators and nucleotide metabolism in antibiotic tolerance in *Escherichia coli*. *Antimicrob Agents Chemother* 52, 2718–2726.

23. Potrykus K & Cashel M (2008) (p)ppGpp: still magical? *Annu Rev Microbiol* 62, 35–51.

24. Battesti A & Bouveret E (2006) Acyl carrier protein/SpoT interaction, the switch linking SpoT-dependent stress response to fatty acid metabolism. *Mol Microbiol* 62, 1048–1063.

25. Kriel A, Bittner AN, Kim SH, Liu K, Tehranchi AK, Zou WY, Rendon S, Chen R, Tu BP & Wang JD (2012) Direct regulation of GTP homeostasis by (p)ppGpp: A critical

This article is protected by copyright. All rights reserved.

component of viability and stress resistance. *Mol Cell* 48, 231–241.

26. Xiao H, Kalman M, Ikehara K, Zemel S, Glaser G & Cashel M (1991) Residual guanosine 3',5'-bispyrophosphate synthetic activity of relA null mutants can be eliminated by spoT null mutations. *J Biol Chem* 266, 5980–5990.

27. Schreiber G, Metzger S, Aizenman E, Roza S, Cashel M & Glaser G (1991) Overexpression of the relA gene in *Escherichia coli*. *J Biol Chem* 266, 3760–3767.

28. Dennis PP & Nomura M (1974) Stringent control of ribosomal protein gene expression in *Escherichia coli*. *Proc Natl Acad Sci USA* 71, 3819–3823.

29. Dalebroux ZD & Swanson MS (2012) ppGpp: magic beyond RNA polymerase. *Nat Rev Microbiol* 10, 203–212.

30. Imai S, Armstrong CM, Kaeberlein M & Guarente L (2000) Transcriptional silencing and longevity protein Sir2 is an NAD-dependent histone deacetylase. *Nature* 403, 795–800.

31. Linster CL, Schaftingen E Van & Hanson AD (2013) Metabolite damage and its repair or pre-emption. *Nat Chem Biol* 9, 72–80.

32. Galperin MY, Moroz O V., Wilson KS & Murzin AG (2006) House cleaning, a part of good housekeeping. *Mol Microbiol* 59, 5–19.

33. Lambrecht JA, Flynn JM & Downs DM (2012) Conserved YjgF protein family deaminates reactive enamine/imine intermediates of pyridoxal 5′-phosphate (PLP)-dependent enzyme reactions. *J Biol Chem* 287, 3454–3461.

34. McLennan a. G (2006) The Nudix hydrolase superfamily. *Cell Mol Life Sci* 63, 123–143.

35. Guranowski A, Jakubowski H & Holler E (1983) Catabolism of diadenosine 5',5"'-

This article is protected by copyright. All rights reserved.

Accepted Article

P1,P4-tetraphosphate in procaryotes. *J Biol Chem* 258, 14784-14789.

36. Goldenzweig A, Goldsmith M, Hill SE, Gertman O, Laurino P, Ashani Y, Dym O, Unger T, Albeck S, Prilusky J, Lieberman RL, Aharoni A, Silman I, Sussman JL, Tawfik DS & Fleishman SJ (2016) Automated structure- and sequence-based design of proteins for high bacterial expression and stability. *Mol Cell* 63, 337–346.

37. Clark RL & Neidhardt FC (1990) Roles of the two lysyl-tRNA synthetases of *Escherichia coli*: analysis of nucleotide sequences and mutant behavior. *J Bacteriol* 172, 3237–43.

38. Miller AD, Wright M, Boonyalai N, Tanner J a & Hindley a D (2006) The duality of LysU, a catalyst for both Ap(4)A and Ap(3)A formation. *Febs J* 273, 3534–3544.

39. Ito K, Oshima T, Mizuno T & Nakamura Y (1994) Regulation of lysyl-tRNA synthetase expression by histone-like protein H-NS of *Escherichia coli*. *J Bacteriol* 176, 7383–6.

40. Rudolph B, Gebendorfer KM, Buchner J & Winter J (2010) Evolution of *Escherichia coli* for growth at high temperatures. *J Biol Chem* 285, 19029–19034.

41. Hassani M, Saluta M V, Bennett GN & Hirshfield IN (1991) Partial characterization of a lysU mutant of *Escherichia coli* K-12. *J Bacteriol* 173, 1965–70.

42. Hittinger CT & Carroll SB (2007) Gene duplication and the adaptive evolution of a classic genetic switch. *Nature* 449, 677–681.

43. Commans S, Plateau P, Blanquet S & Dardel F (1995) Solution structure of the anticodon-binding domain of *Escherichia coli* lysyl-tRNA synthetase and studies of its interaction with tRNA(Lys). *J Mol Biol* 253, 100–13.

44. Cusack S, Yaremchuk a & Tukalo M (1996) The crystal structures of *T. thermophilus* lysyl-tRNA synthetase complexed with *E. coli* tRNA(Lys) and a *T. thermophilus*

This article is protected by copyright. All rights reserved.

Accepted Article

Accepted Article

tRNA(Lys) transcript: anticodon recognition and conformational changes upon binding of a lysyl-adenylate analogue. *EMBO J* 15, 6321–6334.

45. Ely B & Pittard J (1979) Aromatic amino acid biosynthesis: regulation of shikimate kinase in *Escherichia coli* K-12. *J Bacteriol* 138, 933–943.

46. Canalizo-Herna A, Gilston BA, Wang S, Marcus MD, Swindell EP, Xue Y & Mondrago A (2014) Structural and mechanistic basis of zinc regulation across the *E. coli* Zur regulon. *PLoS Biol* 12, e1001987.

47. Tanner JA, Abowath A & Miller AD (2002) Isothermal titration calorimetry reveals a zinc ion as an atomic switch in the diadenosine polyphosphates*. *J Biol Chem* 277, 3073–3078.

48. Wszelaka-Rylik M & Witkiewicz-Kucharczyk A (2007) Ap4A is not an efficient Zn(II) binding agent. A concerted potentiometric, calorimetric and NMR study. *J Inorg Biochem* 101, 758–763.

49. Blanquet S, Plateau P & Brevet A (1983) The role of zinc in 5',5'-diadenosine tetraphosphate production by aminoacyl-transfer RNA synthetases. *Mol Cell Biochem* 52, 3–11.

50. Fuge EK & Farr SB (1993) AppppA-binding protein E89 is the *Escherichia coli* heat shock protein ClpB. *J Bacteriol* 175, 2321–6.

51. Guo W, Azhar MA, Xu Y, Wright M, Kamal A & Miller AD (2011) Isolation and identification of diadenosine 5',5'''-P1,P4-tetraphosphate binding proteins using magnetic bio-panning. *Bioorg Med Chem Lett* 21, 7175–9.

52. Guranowski A, Just G, Holler E & Jakubowski H (1988) Synthesis of diadenosine 5',5'''-P1,P4-tetraphosphate (AppppA) from adenosine 5'-phosphosulfate and adenosine 5'-triphosphate catalyzed by yeast AppppA phosphorylase. *Biochemistry* 27,

This article is protected by copyright. All rights reserved.

2959–2964.

53. Hedstrom L (2009) IMP Dehydrogenase: structure, mechanism, and inhibition. *Chem Rev* 109, 2903–2928.

54. Baykov AA, Tuominen HK & Lahti R (2011) The CBS domain: A protein module with an emerging prominent role in regulation. *ACS Chem Biol* 6, 1156–1163.

55. Pimkin M & Markham GD (2008) The CBS subdomain of inosine 5'-monophosphate dehydrogenase regulates purine nucleotide turnover. *Mol Microbiol* 68, 342–359.

56. Pimkin M, Pimkina J & Markham GD (2009) A regulatory role of the Bateman domain of IMP dehydrogenase in adenylate nucleotide biosynthesis. *J Biol Chem* 284, 7960–7969.

57. Alexandre T, Rayna B & Munier-Lehmann H (2015) Two classes of bacterial IMPDHs according to their quaternary structures and catalytic properties. *PLoS One* 10, e0116578.

58. Yaginuma H, Kawai S, Tabata K V, Tomiyama K, Kakizuka A, Komatsuzaki T, Noji H & Imamura H (2014) Diversity in ATP concentrations in a single bacterial cell population revealed by quantitative single-cell imaging. *Sci Rep* 4, 6522.

59. Bennett BD, Kimball EH, Gao M, Osterhout R, Van Dien SJ & Rabinowitz JD (2009) Absolute metabolite concentrations and implied enzyme active site occupancy in *Escherichia coli*. *Nat Chem Biol* 5, 593–599.

60. Labesse G, Alexandre T, Vaupré L, Salard-Arnaud I, Him JLK, Raynal B, Bron P & Munier-Lehmann H (2013) MgATP regulates allostery and fiber formation in IMPDHs. *Structure* 21, 975–985.

61. Torrents E, Grinberg I, Gorovitz-Harris B, Lundström H, Borovok I, Aharonowitz Y,

This article is protected by copyright. All rights reserved.

Accepted Article

Sjöberg BM & Cohen G (2007) NrdR controls differential expression of the *Escherichia coli* ribonucleotide reductase genes. *J Bacteriol* 189, 5012–5021.

62. Mckethan BL & Spiro S (2013) Cooperative and allosterically controlled nucleotide binding regulates the DNA binding activity of NrdR. *Mol Microbiol* 90, 278–289.

63. Hoffmann HJ, Lymen SK, Lu Chi, Petit M & Echols H (1992) Activity of the Hsp70 chaperone complex - DnaK, DnaJ and GrpE - in initiating phage λ DNA replication by sequestering and releasing λ P protein. *Proc Natl Acad Sci USA* 89, 12108–12111.

64. Ofir-Birin Y, Fang P, Bennett SP, Zhang H-M, Wang J, Rachmin I, Shapiro R, Song J, Dagan A, Pozo J, Kim S, Marshall AG, Schimmel P, Yang X-L, Nechushtan H, Razin E & Guo M (2013) Structural switch of lysyl-tRNA synthetase between translation and transcription. *Mol Cell* 49, 30–42.

65. Yoshida A & Dave V (1975) Inhibition of NADP-dependent dehydrogenases by modified products of NADPH. *Arch Biochem Biophys* 169, 298–303.

66. Miller JH (1972) *Experiments in molecular genetics* Cold Spring Harbor Laboratory, Cold Spring Harbor, NY.

67. Baba T, Ara T, Hasegawa M, Takai Y, Okumura Y, Baba M, Datsenko KA, Tomita M, Wanner BL & Mori H (2006) Construction of *Escherichia coli* K-12 in-frame, single-gene knockout mutants: the Keio collection. *Mol Syst Biol* 2, 2006.0008.

68. Datsenko KA & Wanner BL (2000) One-step inactivation of chromosomal genes in *Escherichia coli* K-12 using PCR products. *Proc Natl Acad Sci* 97, 6640–6645.

69. Wellner A, Raitses Gurevich M & Tawfik DS (2013) Mechanisms of protein sequence divergence and incompatibility. *PLoS Genet* 9, e1003665.

70. Wang W & Malcolm BA Two-stage PCR protocol allowing introduction of multiple

This article is protected by copyright. All rights reserved.

Accepted Article

mutations, deletions and insertions using QuikChange site-directed mutagenesis. *Biotechniques* 26, 680–682.

71. Bronnikov GE & Zakharov SD (1983) Microquantitative determination of Pi-ATP and ADP-ATP exchange kinetics using thin-layer chromatography on silica gel. *Anal Biochem* 131, 69–74.

72. Rockah-Shmuel L, Tawfik DS & Goldsmith M (2014) Generating targeted libraries by the combinatorial incorporation of synthetic oligonucleotides during gene shuffling (ISOR). In *Directed Evolution Library Creation: Methods and Protocols* (Gillam MJE, Copp NJ, & Ackerley D, eds), pp. 129–137. Springer New York, New York, NY.

73. Bennett BD, Yuan J, Kimball EH & Rabinowitz JD (2008) Absolute quantitation of intracellular metabolite concentrations by an isotope ratio-based approach. *Nat Protoc* 3, 1299–311.

74. Kubitschek HE & Friske JA (1986) Determination of bacterial cell volume with the Coulter Counter. *J Bacteriol* 168, 1466–1467.

75. Shalit T, Elinger D, Savidor A, Gabashvili A & Levin Y (2015) MS1-based label-free proteomics using a quadrupole orbitrap mass spectrometer. *J Proteome Res* 14, 1979–1986.

76. Keller A, Nesvizhskii AI, Kolker E & Aebersold R (2002) An explanation of the Peptide Prophet algorithm developed. *Anal Chem* 74, 5383–5392.

77. Murgha YE, Rouillard J-M & Gulari E (2014) Methods for the preparation of large quantities of complex single-stranded oligonucleotide libraries. *PLoS One* 9, e94752.

78. Hensley MP, Gunasekera TS, Easton JA, Sigdel TK, Sugarbaker SA, Klingbeil L, Breece RM, Tierney DL & Crowder MW (2012) Characterization of Zn(II)-responsive ribosomal proteins YkgM and L31 in *E. coli*. *J Inorg Biochem* 111, 164–172.

This article is protected by copyright. All rights reserved.

Accepted Article

Accepted Article

79. Graham AI, Hunt S, Stokes SL, Bramall N, Bunch J, Cox AG, Mcleod CW & Poole RK (2009) Severe zinc depletion of *Escherichia coli*: Roles for high affinity zinc binding by ZinT, zinc transport and zinc-independent proteins. *J Biol Chem* 284, 18377–18389.

80. Patzer SI & Hantke K (1998) The ZnuABC high-affinity zinc uptake system and its regulator Zur in *Escherichia coli*. *Mol Microbiol* 28, 1199–1210.

81. Baker TI & Crawford IP (1966) Anthranilate Synthetase: Partial purification and some kinetic studies on the enzyme from *Escherichia coli*. *J Biol Chem* 241, 5577–5584.

82. Crawford IP & Yanofsky C (1958) On the separation of the tryptophan synthetase of *Escherichia coli* into two protein components. *Proc Natl Acad Sci USA* 44, 1161–1170.

83. Dusha I & Dénes G (1976) Purification and properties of tyrosine-sensitive 3-deoxy-d-arabino-heptolosonate-7-phosphate synthetase of *Escherichia coli* K12. *Biochim Biophys Acta - Enzymol* 438, 563–573.

84. Pittard J & Wallace BJ (1966) Distribution and function of genes concerned with aromatic biosynthesis in *Escherichia coli*. *J Bacteriol* 91, 1494–1508.

85. Huisman GW & Kolter R (1994) Sensing starvation: a homoserine lactone--dependent signaling pathway in *Escherichia coli*. *Science (80-)* 265, 537 LP-539.

86. Schaup HW, Sogin ML, Kurland CG & Woese CR (1973) Localization of a binding site for ribosomal protein S8 within the 16S ribosomal ribonucleic acid of *Escherichia coli*. *J Bacteriol* 115, 82–87.

87. Pon C, Calogero R & Gualerzi C (1988) Identification, cloning, nucleotide sequence and chromosomal map location of hns, the structural gene for *Escherichia coli* DNA-binding protein H-NS. *Mol Gen Genet* 212, 199–202.

88. Deuerling E, Schulze-Specking A, Tomoyasu T, Mogk A & Bukau B (1999) Trigger

This article is protected by copyright. All rights reserved.

factor and DnaK cooperate in folding of newly synthesized proteins. *Nature* 400, 693–696.

89. Kohno K, Wada M, Kano Y & Imamoto F (1990) Promoters and autogenous control of the *Escherichia coli* hupA and hupB genes. *J Mol Biol* 213, 27–36.

90. Terhorst C, Moller W, Laursen R & Wittmann-Liebold B (1973) The primary structure of an acidic protein from 50-S ribosomes of *Escherichia coli* which is involved in GTP hydrolysis dependent on elongation factors G and T. *Eur J Biochem* 34, 138–152.

Supporting information

Table S1. Primers used for generation and cloning in pET_21a of LysU library.

Table S2. Primers used for cloning.

Tables

Table 1. Ap4A intracellular concentrations in the generated *E. coli* K12 strains. Cells were grown in M9-Glc medium for 24 h, diluted 100-fold in fresh M9-Glc, grown and pelleted at the exponential phase. Measurements of Ap4A concentrations were done in duplicate and mean values with standard deviation are presented.

#	Strain	Description	Ap4A (µM)
1	Parental strain *E. coli* K12 MG1655	K12 (wild type)	0.2 ± 0.1
2	Knockout of Ap4A hydrolase	K12 *ΔapaH*	63.6 ± 1.9
	Strains where *apaH's* ORF was exchanged with ORFs of the denoted Ap4A hydrolase variants plus a Tet^R cassette		

This article is protected by copyright. All rights reserved.

3	K12 *ΔapaH*::*apaH*	Wild type *E. coli* ApaH	0.2 ± 0.0
4	K12 *ΔapaH*::*apa*2	*S. cerevisiae* Ap4A phosphorylase	< 0.02
5	K12 *ΔapaH*::*apaH_D7*	A computationally designed ApaH variant with higher thermostability	0.1 ± 0.0
6	K12 *ΔapaH*::*apaH_D7 H120A*	An active-site mutation, H120A, yielding an inactive ApaH	72.0 ± 3.5
7	K12 *ΔapaH*::*apaH_D7 H227A*	An active-site mutation, H227A, with > 200 fold decreased Ap4A hydrolase activity	78.1 ± 19.9
	Strains with pZA plasmid expression of LysU variants		
8	K12; pZA_LysU	Wild type LysU	0.8 ± 0.1
9	K12; pZA_InT	An inactive variant of LysU	0.2 ± 0.1
10	K12; pZA_ LysU_Ap4Asynth	A LysU variant with increased Ap4A synthetase activity and abolished aminoacylation	0.9 ± 0.1
11	K12 *ΔapaH*; pZA_LysU	As # 8 at *ΔapaH* background	62.9 ± 12.5
12	K12 *ΔapaH;* pZA_InT	As # 9 at *ΔapaH* background	58.8 ± 10.7
13	K12 *ΔapaH;* pZA_LysU_Ap4Asynth	As # 10 at *ΔapaH* background	59.5 ± 15.9

Accepted Article

This article is protected by copyright. All rights reserved.

Table 2. High Ap4A levels do not cause cell death. *E. coli* K12 WT and *ΔapaH* cell pre-cultures were adjusted to OD 0.2 and further diluted 100-fold in LB media and incubated at 46 °C. Every hour, 250 µl aliquots of 10^{-4} dilutions of these cultures were plated on LB agar, and the number of colonies was counted after overnight growth at 37 °C. Experiments were done in duplicates and the mean values and standard deviations are presented.

Time (h)	**Wild type (cells/ml * 10^6)**	***ΔapaH* (cells/ml * 10^6)**
0	1.88 ± 0.28	1.30 ± 0.14
1	3.42 ± 0.08	1.08 ± 0.17
2	16.08 ± 0.06	1.34 ± 0.48
3	41.60 ± 4.63	1.54 ± 0.28
4	54.00 ± 8.49	1.04 ± 0.28
5	180.00 ± 33.94	0.72 ± 0.06

This article is protected by copyright. All rights reserved.

Table 3: Proteins down-regulated in *E. coli* K12 *ΔapaH* during exponential growth in M9-Glc.

Name	WT/*ΔapaH* ratio, (number of identified peptides)	Notes
50S ribosomal protein L31 type B, YkgM	4-8, (3-7)	A paralog of L31, a 50S ribosomal subunit protein, that lost the metal-binding "zinc ribbon" motif; may take over L31's function at low zinc [78]
Metal-binding protein, ZinT	2-6, (4-10)	Binds divalent metal ions (Zn^{2+}, Cd^{2+}, Ni^{2+}) and is up-regulated in response to low zinc [79]
High-affinity zinc uptake system protein, ZnuA	4-13, (8-16)	Zn^{2+}-binding component of ABC transporter [80]
Anthranilate synthase component 1, TrpE	2-7, (11-21)	Biosynthesis of tryptophan [81]
Tryptophan synthase alpha chain, TrpA	2-4, (9-18)	Biosynthesis of tryptophan [82]
Phospho-2-dehydro-3-deoxyheptonate aldolase, AroF	3-4, (14-21)	Biosynthesis of aromatic amino acids [83]
T-protein, TyrA	2-3, (12-24)	Biosynthesis of aromatic amino acids (tyrosine and phenylalanine) [84]
Starvation-sensing protein, RspA	4-7, (2-7)	Bifunctional dehydratase that utilizes both D-mannonate and D-altronate as substrates [85]
Starvation-sensing protein, RspB	2-3, (3-5)	Predicted Zn^{2+}-dependent oxidoreductase, on the same operon with rspA [85]

Accepted Article

This article is protected by copyright. All rights reserved.

Table 4. Putative Ap4A binding proteins identified by pull-downs.

Protein name	Enrichment in bioAp4A samples (number of identified peptides)	Notes
Inosine-5'-monophosphate dehydrogenase (IMPDH), GuaB	50-120 (28-53)	Catalyzes the first step in *de novo* guanine biosynthesis [53]
Transcriptional repressor, NrdR	3-68, (4-9)	Zinc-finger/ATP transcriptional regulatory protein, regulates the expression of ribonucleotide reductases (RNRs) [61]
30S ribosomal protein S8, RpsH	2-6, (3-5)	Functions in the post-transcriptional regulation of the ribosomal protein genes [86]
DNA-binding protein, H-NS	2-12, (6-9)	Regulates 5% of all *E. coli* genes and has a key role in bacterial chromosome organization [87]
Chaperone protein, DnaK	~2, (6-64)	The Hsp70 chaperone in *E. coli*. Contributes to control of the heat shock. Also involved in the initiation complex at the viral origin of replication *ori*-λ [88]
DNA-binding protein HU-beta, HupB	2-3, (2)	β-subunit of HU transcriptional regulator, small DNA-binding protein that is considered a global regulatory protein [89]
50S ribosomal protein L7/L12, RplL	2-4, (3-5)	50S ribosomal subunit protein [90]

Accepted Article

This article is protected by copyright. All rights reserved.

Accepted Article

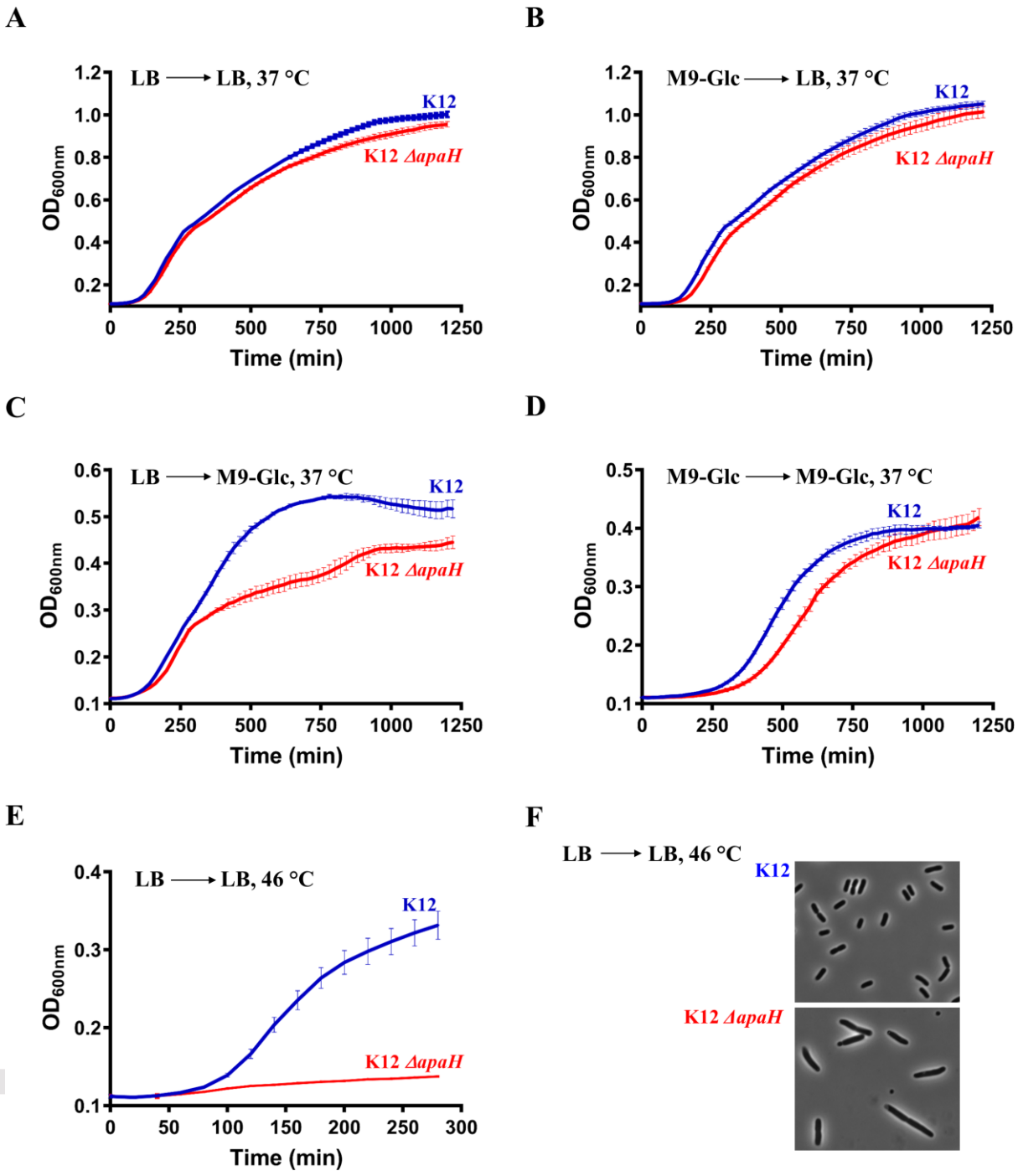

Figure 1. Phenotypic characterization of the *apaH* knockout alongside the parental *E. coli* K12 strain. Cells grown to late stationary phase. This pre-culture was diluted to OD_{600nm} = 0.2 and transferred at 50-fold dilution to a fresh medium. **(A)** LB pre-culture transferred to LB, growth at 37 °C. **(B)** M9-Glc pre-culture transferred to in LB, growth at 37 °C. **(C)** LB

This article is protected by copyright. All rights reserved.

pre-culture transferred to M9-Glc, growth at 37 °C. **(D)** M9-Glc pre-culture transferred to M9-Glc, growth at 37 °C. **(E)** Growth in LB at 46 °C. **(F)** Light microscopy image after 4h growth in LB at 46 °C. All growth experiments were done in 4 repeats and the mean OD_{600nm} values with standard deviation are presented.

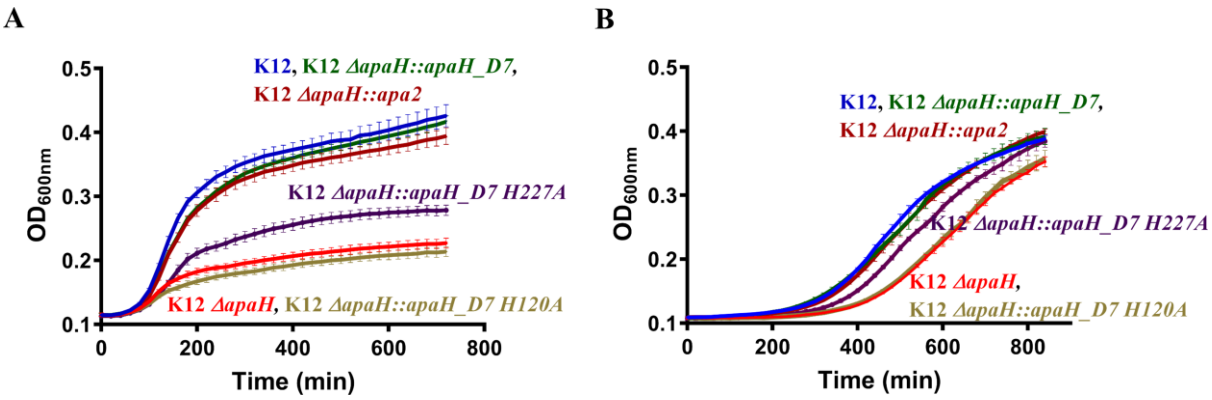

Figure 2. Replacements of ApaH have no growth effect as long as Ap4A is effectively removed. Shown are growth curves in LB at 46 °C **(A)** and M9-Glc at 37 °C **(B)**. Ap4A levels of these strains are provided in Table 1. Chromosomal replacements of ApaH (open reading frame only) with yeast Apa2, a stabilized ApaH variant (ApaH_D7), and ApaH mutants with impaired enzymatic activity. Growth experiments were done in 4 repeats and the mean OD_{600nm} values with standard deviation are presented.

This article is protected by copyright. All rights reserved.

Accepted Article

Accepted Article

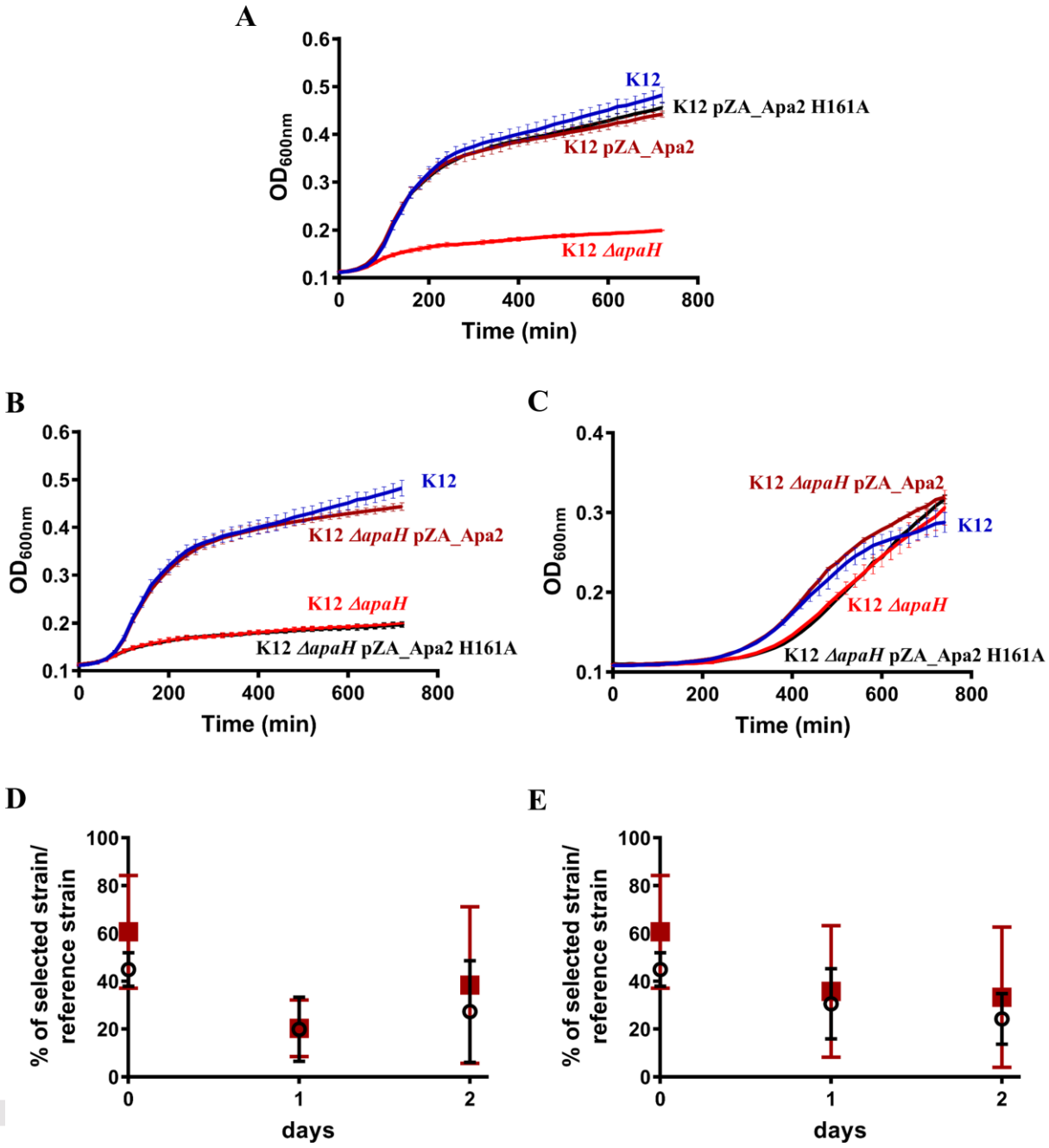

Figure 3. Decrease of Ap4A levels below wild-type's level has no fitness effect. (A) Plasmid expression of Apa2, or its enzymatically inactive mutant (H161A), in the wild type strain in LB at 46 °C. **(B)** Plasmid expression of Apa2, or its enzymatically inactive mutant (H161A), in *ΔapaH* strain in LB at 46 °C and **(C)** in M9-Glc at 37 °C. **(D, E)** Growth

This article is protected by copyright. All rights reserved.

competitions between *E. coli* K12 expressing an active yeast Apa2 and the same strain with an inactive Apa2 control. Cells were mixed at equal ratios and this inoculate was grown over 48 h at 37 °C in LB medium **(D)** and M9-Glc medium **(E)**. The ratio of the competing strain (active yeast Apa2; undetectable Ap4A levels) over the control strain (inactive Apa2; WT-like Ap4A levels) is indicated in dark red squares. These ratios are essentially identical to those seen in a parallel competition of a K12 strain carrying a chloramphenicol resistance marker with an identical strain with no such marker (black circles). All growth experiments were done in 3 repeats and the mean values with standard deviation are presented.

Accepted Article

This article is protected by copyright. All rights reserved.

Accepted Article

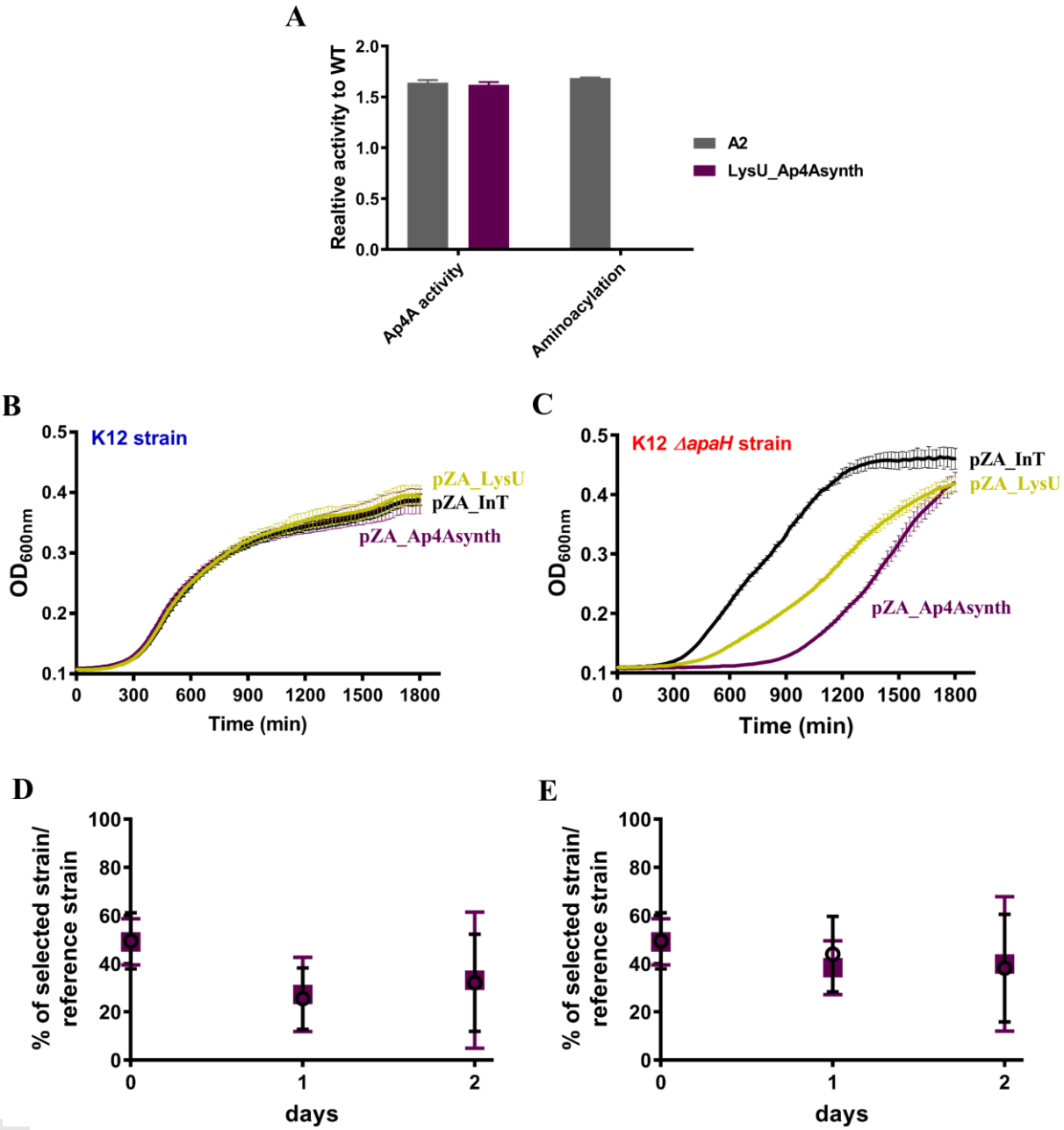

Figure 4. Artificially induced Ap4A production has no observable phenotype. (A) Ap4A synthetase and aminoacylation activities of LysU evolved variants, LysU_A2 and LysU_Ap4Asynth, compared to wild-type LysU. Measurements were done in duplicate and ratio of the mean values with standard deviations are presented. **(B)** Induced expression of LysU in *E. coli* K12 has no growth effect, regardless if wild-type LysU is expressed, or

This article is protected by copyright. All rights reserved.

LysU-inactive (InT), or the engineered Ap4A synthase, LysU_Ap4Asynth. Shown is growth in M9-Glc at 37 °C; identical growth of these strains was also seen at 46 °C. **(C)** Growth effects in M9-Gl at 37 °C were observed in the *ΔapaH* strain and upon induction of LysU expression with AHT. Wild-type LysU, but not its inactivated mutant, InT, caused a lag phase that was further elongated by the engineered Ap4A synthetase variant LysU_Ap4Asynth. **(D, E)** Growth competitions between an *E. coli* K12 strain expressing the Ap4A producing LysU variant and a control strain expressing a LysU inactive variant over 48 h at 37 °C in LB medium **(D)** and M9-Glc medium **(E)**. The ratio of the competing strain (~4.5-fold higher Ap4A levels) over the control strain (WT-like Ap4A levels) is indicated in purple squares, and the control competition is indicated in black circles. Growth experiments were done in 3 repeats and the mean values with standard deviation are presented.

Accepted Article

This article is protected by copyright. All rights reserved.

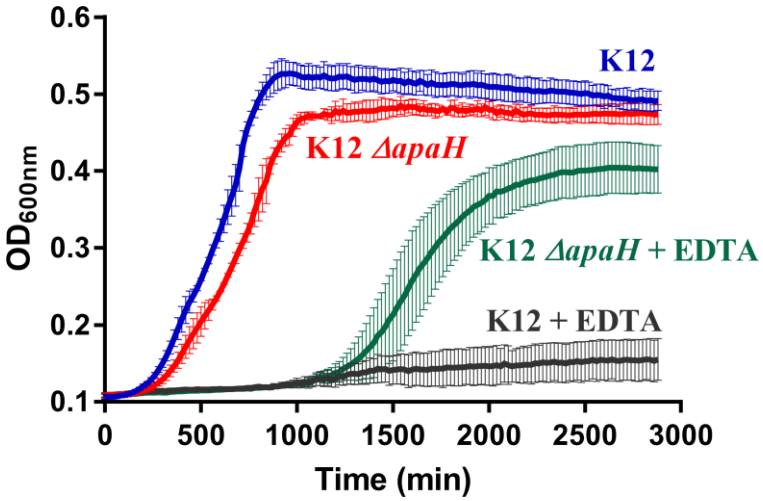

Figure 5. Elevated Ap4A levels enable growth under Zn^{2+} deprivation. Growth of the parental *E. coli* K12 and the *ΔapaH* strain at 37 ºC in M9-Glc, and in same medium supplemented with 0.2 mM EDTA. Growth experiments were done in 3 repeats and the mean OD_{600nm} values with standard deviation are presented.

This article is protected by copyright. All rights reserved.

Accepted Article

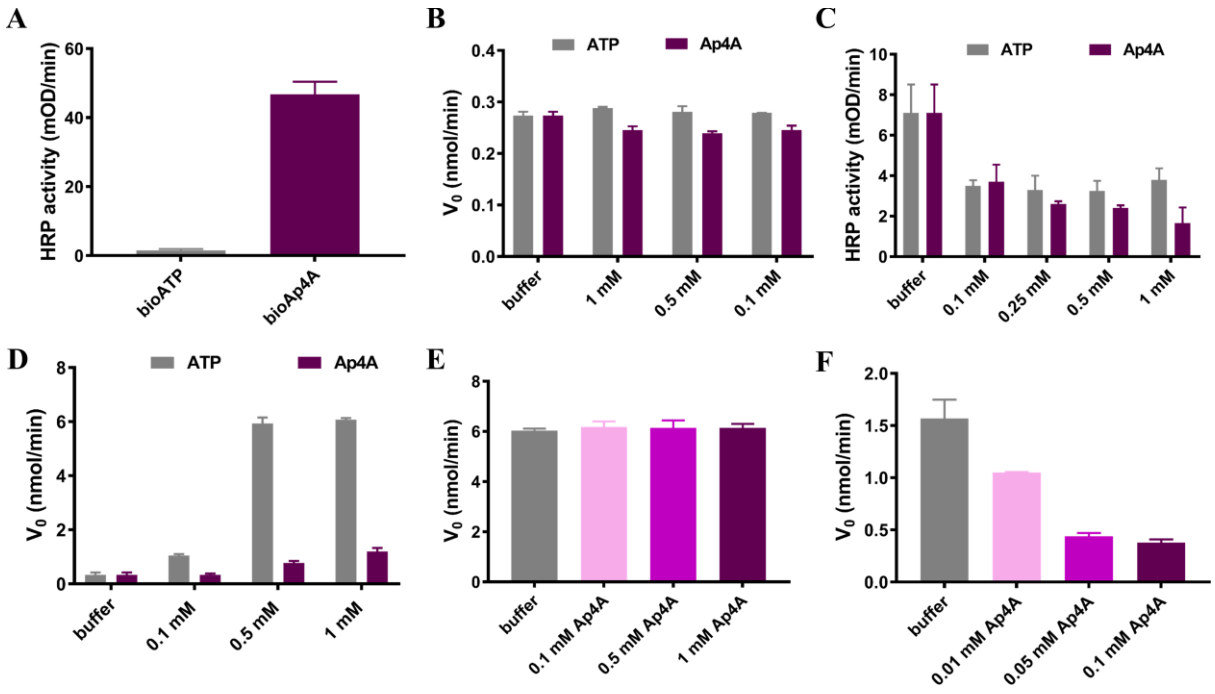

Figure 6. The effects of ATP and Ap4A on the catalytic and regulatory activity of IMPDHs. (A) Binding of *E. coli* IMPDH (*ec*IMPDH) to biotinylated ATP and Ap4A was determined by ELISA (coating ligands onto streptavidin coated plates, and detection of His-tagged IMPDH with anti-His antibodies). **(B)** The enzymatic activity of *ec*IMPDH in the presence of ATP and Ap4A. (Shown are initial rates of NAD^+ reduction, at [IMPDH] = 2 µM; $[IMP]_0$ = 2 mM; $[NAD^+]_0$ = 1 mM.) **(C)** Binding of *ec*IMPDH to ssDNA in the presence of various concentrations of ATP and Ap4A. (Measured as in part A, with an immobilized 5'-biotinylated 300 nt long ssDNA that includes the *gsk* gene promoter region). **(D)** The enzymatic activity of *pa*IMPDH in the presence of varying concentrations of ATP and Ap4A (measured as in part B). **(E)** The enzymatic activity of *pa*IMPDH in the presence of 1 mM ATP and different Ap4A concentrations. **(F)** The enzymatic activity of *pa*IMPDH in the presence of 0.1 mM ATP and different Ap4A concentrations. All the measurements were done in 3 repeats and the mean values with standard deviation are presented.

This article is protected by copyright. All rights reserved.

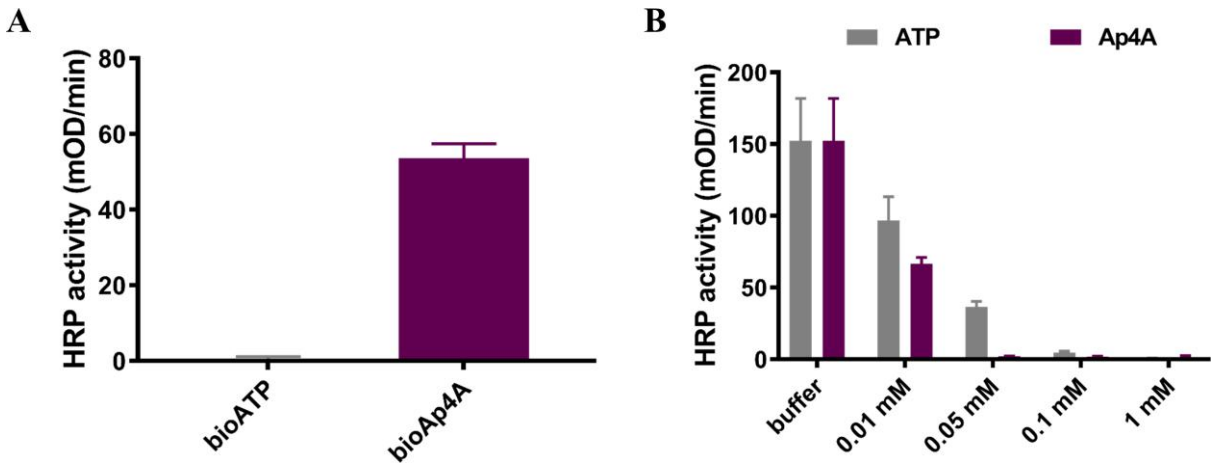

Figure 7. NrdR binding of Ap4A and ATP. (A) Binding of *E. coli* NrdR to biotinylated ATP and Ap4A (determined by ELISA; as in Fig. 6A). **(B)** NrdR binding to the *nrdA* promoter is inhibited by both ATP and Ap4A. All the measurements were done in 3 repeats and the mean values with standard deviation are presented.

Accepted Article

This article is protected by copyright. All rights reserved.